MEMBRANE FOULING DURING THE MICROFILTRATION OF PRIMARY AND SECONDARY WASTEWATER TREATMENT PLANT EFFLUENTS

by

Huifeng Shan

Bachelor of Engineering, East China University of Science and Technology, 1995

Master of Engineering, National University of Singapore, 2002

Submitted to the Graduate Faculty of

School of Engineering in partial fulfillment

of the requirements for the degree of

Master of Science

University of Pittsburgh

2004

UNIVERSITY OF PITTSBURGH

SCHOOL OF ENGINEERING

This thesis was presented

by

Huifeng Shan

It was defended on

May 18, 2004

and approved by

Ronald D. Neufeld, Professor, Civil and Environmental Engineering Department

Leonard W. Casson, Associate Professor, Civil and Environmental Engineering Department

Robert Ries, Assistant Professor, Civil and Environmental Engineering Department

Thesis Advisor: Ronald D. Neufeld, Professor, Civil and Environmental Engineering Department

MEMBRANE FOULING DURING THE MICROFILTRATION OF PRIMARY AND SECONDARY WASTEWATER TREATMENT PLANT EFFLUENTS

Huifeng Shan, MS

University of Pittsburgh, 2004

Microfiltration (MF) has emerged as a useful process for concentrating fine particles and clarifying wastewater. The loss of membrane flux due to fouling, however, is one of the main impediments in the economical development of membrane processes for use in water and wastewater treatment. The nature and extent of fouling when used for wastewater is strongly influenced by three factors: biomass characteristics, operation conditions, and membrane characteristics.

This study is an extension of a previous research [Modise, 2003] on the application of microfiltration in treating combined sewage overflow (CSO) and focused on the fouling mechanism of microfiltration of primary effluent and secondary effluent from municipal wastewater treatment plants, the former of which was used herein to simulate CSO. A 3-step test was designed to fractionate membrane, cake and irreversible fouling resistances in membrane filtration using a stirred dead-end cell system. The results show that the dominating fouling mechanism for microfiltration of primary / secondary effluents is cake resistance. Irreversible fouling dominates the fouling of tap water filtration, indicating a totally different fouling pattern although waste tap water is regarded as one of the major components of municipal wastewater.

The suspended solids in both primary and secondary effluents were investigated to be moderately compressible particles by showing a compressibility index n around 0.4-0.6.

The irreversible fouling of membrane filtration, as the term suggests, is hard to remove and results in unrecoverable permeate flux decline in practice although it occupies a comparatively smaller fraction of the total hydraulic resistances in sewage effluent filtration than deposited cake. A multi-cycle test was conducted to investigate how the irreversible resistance will vary over repeated cycles of membrane filtration and surface cleaning like a long-term practical application. The result of a 17-cycle test showed that the irreversible resistance gradually increased from initial 5% to about 21% of total resistance after six cycles and then basically remained constant at this plateau. This study is valuable to industrial application and design of membrane processes, especially in the application of microfiltration of CSO or primary/secondary effluents as a tertiary treatment method.

TABLE OF CONTENTS

ACKNOWLEDGEMENTS xvi

INTRODUCTION 1

1.0 LITERATURE REVIEW 3

1.1 APPLICATION OF MICROFILTRATION IN WATER TREATMENT 3

1.1.1 Key characteristics of membranes and their application 3

1.1.1.1 Hydrophilicity vs. hydrophobicity 3

1.1.1.2 Surface charge 4

1.1.1.3 Membrane modification 4

1.1.2 Fouling 5

1.1.2.1 Fouling in MF and UF 5

1.1.2.2 Biofouling 7

1.1.2.3 Formation of a dynamic membrane by mixed liquor suspended solids (MLSS) 8

1.1.3 Effect of backpulsing on mitigating membrane fouling 9

1.2 THEORY FOR DEAD-END MICROFILTRATION 10

1.2.1 Dead-end flux mechanisms 10

1.2.2 Theory for dead-end microfiltration 14

1.2.2.1 Membrane resistance 14

1.2.2.2 Cake resistance 16

1.2.3 Cake compressibility 17

1.2.4 Properties of compressible cake 19

1.2.5 Dynamic simulation/analysis of cake properties 21

1.2.6 Experimental method to measure cake porosity and thickness 24

1.3 SPECIFIC CAKE RESISTANCE OF ACTIVATED SLUDGE 25

1.4 CRITICAL FLUX 26

1.5 EXPERIMENTAL METHOD TO DIFFERENTIATE HYDRAULIC RESISTANCES 27

1.6 FRACTIONATION OF FOULANTS IN NATURAL WATER 28

1.7 FEASIBILITY OF USING MEMBRANE FILTRATION AS TERTIARY TREATMENT TECHNOLOGY 28

1.8 MICROFILTRATION/ULTRAFILTRATION OF PRIMARY OR SECONDARY EFFLUENTS 29

2.0 MATERIALS AND METHODS 31

2.1 EXPERIMENTAL SET UP 31

2.2 FEEDWATER 32

2.3 WATER QUALITY ANALYSIS 33

2.4 MEMBRANES 33

2.5 DATA RECORDING AND PROCESSING 34

2.6 FRACTIONATE MEMBRANE, CAKE AND IRREVERSIBLE RESISTANCES BY A 3-STEP TEST 35

2.7 SPECIFIC CAKE RESISTANCE (α) AND COMPRESSIBILITY INDEX N 36

2.8 COMPARISON AMONG DIFFERENT CLEANING METHODS IN STEP 3 OF THE 3-STEP TEST 38

2.9 IRREVERSIBLE FOULING: A MULTI-CYCLE TEST OF PRIMARY EFFLUENT USING VERSAPOR MEMBRANE 38

3.0 RESULTS AND DISCUSSION 40

3.1 FRACTIONATE HYDRAULIC RESISTANCES 41
3.1.1 Microfiltration of primary effluent 41
3.1.2 Microfiltration of secondary effluent 48
3.1.2.1 Filtration of secondary effluent sampled in a wet vs. dry weather day 48
3.1.2.2 Comparison between Supor and Versapor in secondary effluent filtration 51
3.2 SPECIFIC CAKE RESISTANCE (α) AND COMPRESSIBILITY INDEX N 54
3.2.1 Primary effluent 55
3.2.2 Secondary effluent 58
3.3 FILTRATION OF TAP WATER AND DI WATER 61
3.3.1 Tap water filtration 61
3.3.2 DI water filtration 66
3.4 COMPARE DIFFERENT CLEANING METHODS TO REMOVE CAKE RESISTANCE R_c 67
3.5 MULTI-CYCLE TEST OF PRIMARY EFFLUENT 72
3.6 COMPARISON BETWEEN EXPERIMENTAL DATA AND THE LITERATURE 80
4.0 SUMMARY AND CONCLUSIONS 83
5.0 SUGGESTIONS FOR FURTHER STUDIES 86
APPENDIX A 88
DERIVATIONS OF W AND α 88
APPENDIX B 92
SAMPLE CALCULATION OF THE FLUX RESISTANCES IN THE 3-STEP TEST 92
APPENDIX C 93
MEASUREMENT OF SPECIFIC CAKE RESISTANCE (α) FOR PRIMARY EFFLUENT 93
APPENDIX D 97

MEASUREMENT OF SPECIFIC CAKE RESISTANCE (α) FOR SECONDARY EFFLUENT 97

APPENDIX E 101

INFLUENCE OF PHYSICAL ABRASION OF MEMBRANE ON RESTORING PERMEATE FLUX 101

BIBLIOGRAPHY 103

NOMENCLATURE

α specific cake resistance on a mass basis

$\hat{\alpha}$ specific cake resistance per unit thickness

μ or η_0 viscosity of water

δ_c cake thickness

ε_c the void fraction of the cake

δ_m or L membrane thickness

ε_m porosity of membrane ≡ the membrane void volume/total volume

ΔP transmembrane pressure

ρ_s the mass density of the solids comprising the cake

A the area of the membrane

C_b the concentration of SS of the feedwater

d_p particle diameter

J_0 the initial filtration flux through the clean membrane

J_v or J filtration flux rate

K_c cake permeability

n cake compressibility index

N number of open pores

N_0 the initial pore density

n_p the number of pores per unit area

P_s compressive drag pressure in the solids

P_x hydraulic pressure

R_c cake resistance

R_i irreversible resistance

R_m membrane resistance

r_p radius of the membrane pores

S_c the solids surface area per unit volume of solids in the cake

S_m specific surface area ≡ pore surface area/solids volume

V volume of filtrate

w the mass of cake deposited per unit area of membrane

LIST OF TABLES

Table 1 Technical specification of Versapor®-200 w/wa 0.2 μm and Supor®-200 0.2 μm membranes [Pall website] 34

Table 2 Summary of hydraulic resistances and their respective significance in filtration of primary effluent using Versapor and Supor membrane 43

Table 3 Summary of hydraulic resistances and their respective significance for (a) dry weather secondary effluent using Versapor membrane, (b) wet weather and (c) dry weather secondary effluent using Supor membrane 49

Table 4 Compressibility indices of selected microorganisms and particles [Nakanishi, et al. 1987]..... 55

Table 5 Comparison between the suspended solids concentrations of the sewage effluent samples and the the corresponding daily and monthly average SS data provided by the analytical lab of Alcosan 57

Table 6 Specific cake resistance (α) values under different pressures for primary effluent 57

Table 7 Specific cake resistance α values under different pressures for secondary effluent ... 59

Table 8 Relative contribution to flux resistance for tap water filtration with Supor membrane 64

Table 9 Suspended solids and volatile suspended solids in primary and secondary effluents, and tap water 65

Table 10 Influence of physical abrasion of membrane on restoring permeate flux..... 71

Table 11 Summary of data of multi-cycle experiments..... 74

Table 12 Comparison of published sludge filtration data with this study 82

Table 13 Raw data of filtration of primary effluent with transmembrane pressure of 10 psi..... 93

Table 14 Raw data of filtration of primary effluent with transmembrane pressure of 15 psi..... 94

Table 15 Raw data of filtration of primary effluent with transmembrane pressure of 20 psi..... 95

Table 16 Raw data of filtration of secondary effluent with transmembrane pressure of 10 psi. 97

Table 17 Raw data of filtration of secondary effluent with transmembrane pressure of 15 psi. 98

Table 18 Raw data of filtration of secondary effluent with transmembrane pressure of 20 psi. 99

LIST OF FIGURES

Figure 1 Conceptual illustration of membrane fouling (a) without and (b) with dynamic membrane [Lee et al., 2001] 9

Figure 2 Comparison of pore blockage, pore constriction, and cake formation models. Upper panel shows the normalized resistance, lower panel shows normalized flux. [Zeman and Zydney, 1996] 13

Figure 3 Ratio of filtration time (t) and filtrate volume (V) as a function of filtrate volume (V). MFI determined from the gradient slope of the linear portion of the t/V vs. V plot [Boerlage, et al., 2003]..... 19

Figure 4 Filtration curve of dt/dV vs. V for Dextran-MnO_2 colloids under Δp = 200 kPa, where I, II and III stands for stage I (particle deposition), II (cake compression) and III (loose packing of newly formed cake) respectively. [Hwang and Hsueh, 2003] 23

Figure 5 Experimental set up of the dead-end stirred cell system 32

Figure 6 Fractionation of hydraulic resistances in filtration of primary effluent. R_c – cake resistance, R_i – irreversible resistance, R_m – membrane resistance. 44

Figure 7 Comparison of the flux rates of primary effluent filtration by the 3-step test (I. clean water filtration; II. feed water filtration; III. clean water filtration after membrane surface cleaning) under 15 psi, stirred condition using Versapor membrane and Supor membrane. The dotted line showed how the steady state fluxes were determined. ... 47

Figure 8 Fractionation of hydraulic resistances in filtration of secondary effluent taken in a wet weather day and a dry weather day. R_c – cake resistance, R_i – irreversible resistance, R_m – membrane resistance. 50

Figure 9 Productivities of Versapor and Supor membrane in filtration of secondary effluent taken in dry weather day under15 psi 52

Figure 10 Flux rates of Versapor and Supor membrane in filtration of secondary effluent taken in dry weather day under15 psi..... 53

Figure 11 Summary of plots of t/V vs. V for primary effluent filtrations under different pressures, C_b = 64 mg/l. 56

Figure 12 Summary of plots of t/V vs. V in secondary effluent filtration, C_b = 11 mg/l. 59

Figure 13 Plotting log α vs. log P to get compressibility index n of particles in sewage effluent according to $\alpha = \alpha_0(\Delta p)^n$ 60

Figure 14 Flux decline of tap water in the filtration using Supor membrane 62

Figure 15 Variation in permeate flux of tap water in the step 2 and 3 of the 3-step test (I. DI water filtration; II. feed water filtration; III. DI water filtration after membrane surface cleaning by warm (~38°C) and gentle water flushing (1.5 GPM)) with Supor membrane at 15 psi, flux in step 2 means tap water flux, flux in step 3 means clean water flux of the fouled membrane after cleaning 64

Figure 16 Comparison of the fouling mechanisms of primary/secondary effluents and tap water 65

Figure 17 Flux declines of DI water (left part) and permeate, i.e. filtered DI water (right part) in the filtration using Supor membrane..... 67

Figure 18 Comparison of four cleaning methods to be adopted in step 3 of the s-step test 70

Figure 19 Correlation between suspended solids (SS) and turbidity of primary effluent 73

Figure 20 Comparison of irreversible resistance (R_i) and its fraction to total hydraulic resistance (R_t), i.e. R_i/R_t, in different cycles. The dotted line was added as trend lines..... 75

Figure 21 Summary of variation of stabilized clean water fluxes after membrane surface cleaning in the multi-cycle test. The dotted line was added as trend lines. 76

Figure 22 Control 1 – Effect of soaking a new piece of membrane in DI water on its permeation 78

Figure 23 Control 2 – effect of the cleaning method of hot (53°C) and water flushing (2.9 gpm) on membrane permeation. The abscissa is the accumulative time of water flushing. For example, the 2nd point (t = 10 min) means the membrane was flushed for 10 min for the first time, the 7th point (t = 80 min) means a continuous 30 minutes flushing was applied..... 79

Figure 24 Plotting t/V vs. V to get the slop of the linear phase, which is used to calculate the specific cake resistance α_{10psi} for primary effluent according to the equation $\alpha = \frac{slope \times 2A^2\Delta P}{\mu C_b}$ 94

Figure 25 Plotting t/V vs. V to get the slop of the linear phase, which is used to calculate the specific cake resistance α_{15psi} for primary effluent according to the equation $\alpha = \frac{slope \times 2A^2\Delta P}{\mu C_b}$ 95

Figure 26 Plotting t/V vs. V to get the slop of the linear phase, which is used to calculate the specific cake resistance α_{20psi} for primary effluent according to the equation $\alpha = \frac{slope \times 2A^2\Delta P}{\mu C_b}$ 96

Figure 27 Plotting t/V vs. V to get the slop of the linear phase, which is used to calculate the specific cake resistance α_{10psi} for secondary effluent according to the equation $\alpha = \frac{slope \times 2A^2\Delta P}{\mu C_b}$ 98

Figure 28 Plotting t/V vs. V to get the slop of the linear phase, which is used to calculate the specific cake resistance α_{15psi} for secondary effluent according to the equation $\alpha = \frac{slope \times 2A^2\Delta P}{\mu C_b}$ 99

Figure 29 Plotting t/V vs. V to get the slop of the linear phase, which is used to calculate the specific cake resistance α_{20psi} for secondary effluent according to the equation $\alpha = \frac{slope \times 2A^2\Delta P}{\mu C_b}$ 100

ACKNOWLEDGEMENTS

I'm deeply grateful to my major advisor, Dr. Ronald D. Neufeld as well as Dr. Radisav D. Vidic at the University of Pittsburgh. Without their insightful advice and dedication, this work could not be accomplished. I also give my heartfelt appreciation to my beloved wife, Yue Luo, for her consistent support and encouragement.

INTRODUCTION

Pressure driven membranes are divided into four main divisions based on pore size, i.e. microfiltration (MF), ultrafiltration (UF), nanofiltration (NF) and reverse osmosis (RO) with decreasing pore size. The typical pore size of microfiltration membranes is 0.1 to 2 μm. Typical applied pressure is 15 to 60 psi.

Microfiltration (MF) has emerged as a useful process for concentrating fine particles and clarifying wastewater. It has been demonstrated that microfiltration is applicable in treating domestic wastewater and that the effluent quality can satisfy the requirement for wastewater reuse. The loss of membrane flux due to fouling, however, is one of the main impediments in the economical development of membrane processes for use in water and wastewater treatment. The nature and extent of fouling when used for wastewater is strongly influenced by three factors: biomass characteristics, operation conditions, and membrane characteristics. In general, three fouling mechanisms, i.e. pore blockage, pore constriction and cake formation are simultaneously responsible for membrane fouling. For microfiltration, cake formation is the dominating fouling mechanism.

This study is an extension of a previous research on application of microfiltration in treating combined sewage overflow (CSO) caused by flooding of municipal combined sewage system (CSS) due to heavy rainfall and snowmelt. Direct discharge of CSO into surface water may

result in environmental pollution, which will lead to health hazards to human and animals. Microfiltration of CSO can provide a solution of this problem. This study focuses on the fouling mechanism of microfiltration of primary effluent and secondary effluent from municipal wastewater treatment plants, the former of which was used herein to simulate CSO. A 3-step test was designed to fractionate membrane, cake and irreversible resistances in membrane filtration of primary and secondary effluents using a stirred dead-end cell system, aiming at investigating their respective significance to the membrane fouling and which is the dominating mechanism. Taking into account that waste tap water is a major component of municipal wastewater, the fouling mechanism of clean tap water in microfiltration was also studied and compared to those of sewage effluents.

The irreversible fouling of membrane filtration of sewage effluents is hard to remove and cause an irretrievable membrane flux loss. A multi-cycle test was designed to investigate how the irreversible resistance would vary during repeated cycles of operation. This study will provide referable value to industrial application and design of membrane processes, especially in the application of microfiltration of CSO or primary/secondary effluents as a tertiary treatment method.

1.0 LITERATURE REVIEW

This literature review mainly focused on three aspects, first, the application of microfiltration in treatment of primary and/or secondary effluents from municipal wastewater treatment plants, in which the major impediment of the membrane filtration – fouling was emphasized; second, the dead-end filtration theory, especially the properties of compressible cake; finally, prior experimental methods to fractionate the hydraulic resistances of membrane filtration and foulants.

1.1 APPLICATION OF MICROFILTRATION IN WATER TREATMENT

1.1.1 Key characteristics of membranes and their application

1.1.1.1 Hydrophilicity vs. hydrophobicity

Hydrophilicity means the surface chemistry allows these materials to be wetted forming a water film or coating on their surface. Hydrophobic materials have little or no tendency to adsorb water and water tends to "bead" on their surface. Hydrophilic materials possess an ability to form "hydrogen-bonds" with water. For Microfiltration (MF) membranes, hydrophilicity & hydrophobicity influence wettability and applied pressure requirements for liquid flow through the membrane and adhesion characteristics of contaminants to the

membrane materials. The greater the tendency for a material to associate with water through hydrogen bonding, the more hydrophilic the material is [Rudie].

Hydrophilicity & hydrophobicity of the surface of membranes influence fouling. Many natural products are negatively charged or have partial negative net charge due to dipole or multiple chemical bonds in their structure. Particles that foul membranes in aqueous media tend to be hydrophobic. General tendency will favor particle attachment to any material less hydrophilic than water because less exposure of hydrophobic particles can be achieved by attachment of the particles to the membrane surface. The hydrophobic membranes always exhibit a greater fouling tendency during the membrane filtration of activated sludge than the hydrophilic membrane due to hydrophobic interaction between solutes, microbial cells, and membrane material [Choi et al., 2002; Chang et al., 1999].

1.1.1.2 Surface charge

The membrane appears as if it carries a surface charge. The potential field created by this charge can attract or repel charged species in water. It is generally believed that having a membrane with a negative charge is preferable. [Cardew and Le, 1998].

1.1.1.3 Membrane modification

Membrane surface modification techniques are used to modify membrane hydrophilicity or hydrophobicity, and further yield different response to chemical resistance, fouling and adsorption. Chemical or physical modification of homogeneous membranes can drastically change their intrinsic properties, especially when ionic groups are introduced into the

materials of the membrane surface. These techniques include water insoluble surfactants treatment, coating, chemical grafting, polymer blends and plasma (high energy gas) modification [Rudie]. Several studies have demonstrated the importance of hydrophobility of membrane materials. It is known that hydrophilic membranes yield higher flux because of the hydrophobic nature of the interaction between the membrane and biomass. This demands that the naturally hydrophobic polymeric materials, such as polyethylene, polypropylene, polyvinilydene fluoride, and polysulfone, are surface modified with some hydrophilic functional group [Chang, et al. 2002]. The surface characteristics of both UF and MF membranes can be modified by adsorption with a non-anionic surfactant composed of polyethylated linear aliphatic alcohols, resulting in a significant improvement in oil rejection [Marchese, et al. 2000].

1.1.2 Fouling

1.1.2.1 Fouling in MF and UF

Microfiltration (MF) and ultrafiltration(UF) have emerged as useful processes for concentrating fine particles and clarifying wastewater. Microfiltration is applicable in treating domestic wastewater and the effluent quality can satisfy the requirement for wastewater reuse such as irrigation, toilet flushing, etc. [Alonso et al. 2001; Parameshwaran, et al. 2001; Ahn and Song, 1999].

Cross-flow configuration is a good fluid engineering technique to maintain permeate flux in the majority of membrane filtration application. However, the permeate flux is limited by a layer of particles, colloids or macromolecules that deposit on the membrane surface, rather

than by the resistance to flow through the membrane itself. This built-up layer makes the permeate flux diminish with time and is called fouling. For some microfiltration applications, the reduction in the permeation rate can be severe enough to undermine the inherently high permeability associated with MF membranes and the severe flux decline can often happen during the initial filtration period [Hsieh, 1996].

The nature and extent of fouling are strongly influenced by three factors: biomass characteristics, operation conditions, and membrane characteristics. The membrane characteristics such as pore size, porosity, surface energy, charge, roughness, and hydrophilicity/hydrophobicity, etc. have a direct impact on membrane fouling. Membrane with very smooth surface (and with very small pores) would be expected to "trap" fewer particles than those with surface topographies that have roughness elements (or pores) of the same size as the macrosolutes and particles [Zeman and Zydney, 1996]. Fouling control techniques, which have been investigated, include low-flux operation, high-shear cross flow, periodical air or permeate backflushing, intermittent suction operation or powdered activated cabon (PAC), etc. [Chang, et al. 2002].

Ceramic membrane materials include aluminum, zirconium and titanium oxide (Al_2O_3, ZrO_2, and TiO_2, respectively). Ceramic MF/UF membranes have inherently superior physical integrity, chemical resistance, and thermal stability that render them suitable for extreme-condition application. Ceramic membranes are well suited for slurry filtration, oil-water emulsion separations, surface water filtration, aqueous cleaner recovery, as well as food, dairy and beverage applications [Sondhi and Bhave, 2001].

1.1.2.2 Biofouling

A biofilm is a matrix of cells and cellular products, such as extracellular polysaccharides (EPS) and polypeptides, attached to a solid surface of substratum. Biofilms can present a problem when they occur in unwanted locations such as industrial process equipment or implanted medical devices. Biofouling is the accumulation and possible growth of living organisms and their associated organic material and debris on a surface. In most environments microorganisms prefer to grow as sessile communities and this is likely due to the protective nature of biofilm growth [Walker, et al., 2000]. But these microbial films can also present positive opportunities in bioremediation of hazardous and toxic substances in ground and surface water and wastewater treatment. Biofilm and other immobilized cell reactors offer significant advantages in bioprocessing, such as increased process flow rates without washing the organisms from the reactor [EPA (1992); Hjortso and Roos, 1995].

Biofilms are dynamic microenvironments, encompassing processes such as metabolism, growth, and product formation, and finally detachment, erosion, or "sloughing" of the biofilm from the surface [EPA (1992)]. Biofilm typically accumulate on surfaces exposed to flowing water. The accumulation of microbial film is most likely rate-limited by the transport of nutrients and by-products from the bulk liquid to the biofilm. Cellular attachment to a solid surface provides a suitable environment for many types of microorganisms under varied and sometimes harsh conditions.

Bacterial fouling can be a major problem in many MF/UF systems. The bacterial cell surface consists of a peptidoglycan layer covalently linked to a variety of membrane proteins and anionic polymers. Although much of this outer surface is hydrophilic, many bacterial surfaces

have some hydrophobic characters as well, and are thus able to attach to many polymeric surfaces by strong hydrophobic interaction. In addition, bacteria possess specific lectins and/or adhesins on their outer surfaces which can chemically bind to complementary structures on the surface of different polymeric membranes and/or different adsorbed macromolecules. Many adherent bacteria secrete a variety of exopolysaccharides, which then become part of an extracellular slime or biofilm on the solid surface [Zeman and Zydney, 1996]. Most of the membrane bioreactor (MBR) producing low filtration flux (10-20 l/h.m^2) work in the presence of a "filtration cake" due to the accumulation of bioparticles on the membrane surface. This leads to a rapid increase in membrane hydraulic resistance from the very beginning of the filtration, until the flow rate level off after a few minutes or a few hours [Tardieu, et al., 1998]. Extracellular polymeric substances (EPS) provide a highly hydrated gel matrix in which microorganisms are embedded, they provide a significant barrier to permeate flow in MBR.

1.1.2.3 Formation of a dynamic membrane by mixed liquor suspended solids (MLSS)

Suspended solids could be an important factor affecting membrane permeability because the suspended solids, mainly microbial flocs could form a dynamic membrane, i.e. biofilm, on the surface of membrane. The conceptual illustration of dynamic membrane is shown in Figure 1. Small particles like soluble organics will deteriorate the permeability of membrane by directly adsorbing onto the surface or inside the membrane pores when arriving at the membrane without any interruption. Because low molecular weight substances or submicron colloidal particles could be rejected / sorbed and biodegraded by the dynamic membrane composed of living microorganisms, the dynamic membrane could provide small molecules with fewer

chances of interacting with membranes and thereby alleviate the rate of membrane fouling. Repeated process of formation and removal of dynamic membranes by tangential flow (in this study, it is liquid flow only) may slow down the decline of membrane permeability [Lee et al., 2001].

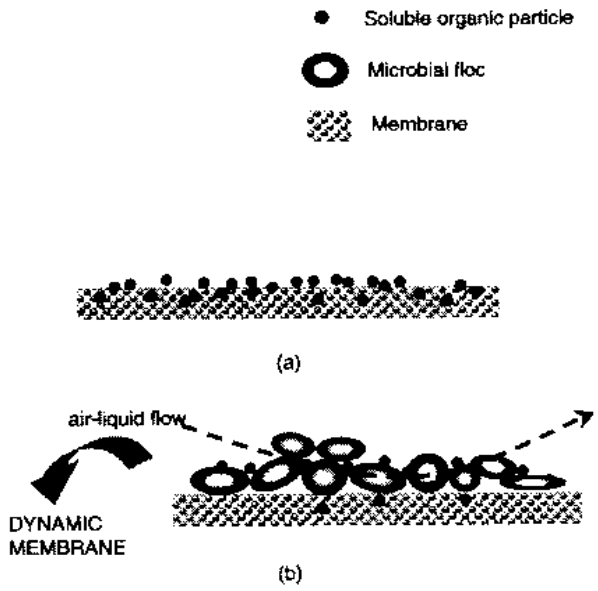

Figure 1 Conceptual illustration of membrane fouling (a) without and (b) with dynamic membrane [Lee et al., 2001]

1.1.3 Effect of backpulsing on mitigating membrane fouling

Transmembrane pressure pulsing or backpulsing (BP) is an effective technique for reducing fouling phenomenon in membranes, improving the overall filtration rate and extending the cleaning interval. [Zhao, et al. 2002; Sondhi and Bhave, 2001]. Several variations of backpulsing exist and they all involve temporary reverse flow of either the permeate or air. Thus, the permeate can be delivered through the membrane from the permeate side to the feed side by applying a momentarily higher pressure on the permeate side or suction on the feed

side. The pressure required for backpulsing to dislodge particles can be several times that of the transmembrane pressure (TMP) difference and increases with increasing number of particle layers accumulated on the membrane surface. This backpulsing often dislodges the deposits on the membrane surface and the loosened deposits are then carried away by the retentate flow. Within each backpulsing cycle, the flux will start to decline and a fresh backpulse is imposed to restore the flux level. Two of the important design parameters of a backpulsing system are the frequency and duration of the pulse employed. An effective strategy of design and operation of backflushing should be to apply more frequent short high-pressure pulse [Hsieh, 1996], say, flow reverse occurs every few minutes and reverse pulses (up to 10 bar) are applied for very short periods of time (typically <1 s) [Sondhi and Bhave, 2001]. Backpulsing is of special significance in ceramic membrane filtration because unlike polymeric membranes, ceramic membranes are able to withstand the high pressure associated with backpulsing.

1.2 THEORY FOR DEAD-END MICROFILTRATION

1.2.1 Dead-end flux mechanisms

Dead-end filtration means the feed water flow is perpendicular to the filter or membrane, whereas the feed water flow in cross-flow filtration is parallel to the membrane. The water is pushed through the membrane by a pressure gradient in both cases. Three separate mechanisms have been used to explain the flux decline associated with particle deposition during membrane filtration: pore blockage, pore constriction and cake filtration. Pore constriction is only possible for membrane with relatively large pores that are easily

accessible to the macrosolutes/particles. Pore blockage and cake formation will thus dominate when the pores are smaller than the particles.

In the pore blockage model, the rate of change in the number of open pores is assumed to be directly related to the rate of particle convection to membrane surface:

$$\frac{dN}{dt} = -\alpha_{block} A J_v C_b \tag{1}$$

where α_{block} provides a measure of the pore blockage efficiency, A is the area of the membrane and C_b is the concentration of SS of the feedwater. Cake formation is assumed to be negligible, i.e. $R_c = 0$. Substitution of Eq. 1 into Darcy's law and Hagen-Poiseuille equation (Eq. 8 and 10) yields upon integration

$$\frac{J_v}{J_0} = \exp(-\frac{\alpha_{block} A J_0 C_b}{N_0} t) \tag{2}$$

where J_0 is the initial filtration flux through the clean membrane and N_0 is the initial pore density.

In the pore constriction model, the rate of change in the (cylindrical) pore volume is assumed to be proportional to the rate of particle convection to the membrane:

$$\frac{d}{dt}(\pi \cdot r_p{}^2 \delta_m) = -\alpha_{pore} A J_v C_b \tag{3}$$

where δ_m is membrane thickness, r_p is the pore radius, yielding

$$\frac{J_v}{J_0} = (1 + \frac{\alpha_{pore} A J_0 C_b}{\pi r_0{}^2 \delta_m} t)^{-2} \tag{4}$$

In the cake filtration model, the hydraulic resistance provides by the particle cake is assumed to be proportional to the cake mass, m_{cake}:

$$R_c = (\frac{\alpha_{cake}}{A}) m_{cake} \tag{5}$$

with the rate of particle deposition directly related to the rate of particle convection:

$$\frac{dm_{cake}}{dt} = AJ_v C_b \tag{6}$$

Substitution of Eq. 5 and 6 into Darcy's law yields

$$\frac{J_v}{J_0} = (1 + \frac{2\alpha_{cake} J_0 C_b}{R_m} t)^{-1/2} \tag{7}$$

All three models predict a quasi-linear flux decline at initially short time, with the steepest decline seen for the cake filtration model. The reverse behavior is seen at extended long times, where the lowest flux is obtained with the pore blockage model (lower panel in Figure 2). At large times, the flux given by the pore blockage model decays exponentially with time. The pore constriction model shows a $(J_v/J_o) \sim t^{-2}$ dependence and the cake filtration model predicts $(J_v/J_o) \sim t^{-1/2}$. The difference in the fouling models becomes much more apparent in the plot of relative resistance, R/R_m, versus time (upper panel in Figure 2). The pore blockage and constriction models both predict that R/R_m increase with increasing time with an increasing slope (concave up) while the cake filtration model predicts that the plot of R/R_m versus t is concave down. These differences can be used to distinguish between internal (pore blockage or pore constriction) and external (cake formation) fouling during filtration. [Zeman and Zydney, 1996]. Most of the derivations of the equations cited in the chapter of literature review are not provided, except for those that are used in the study.

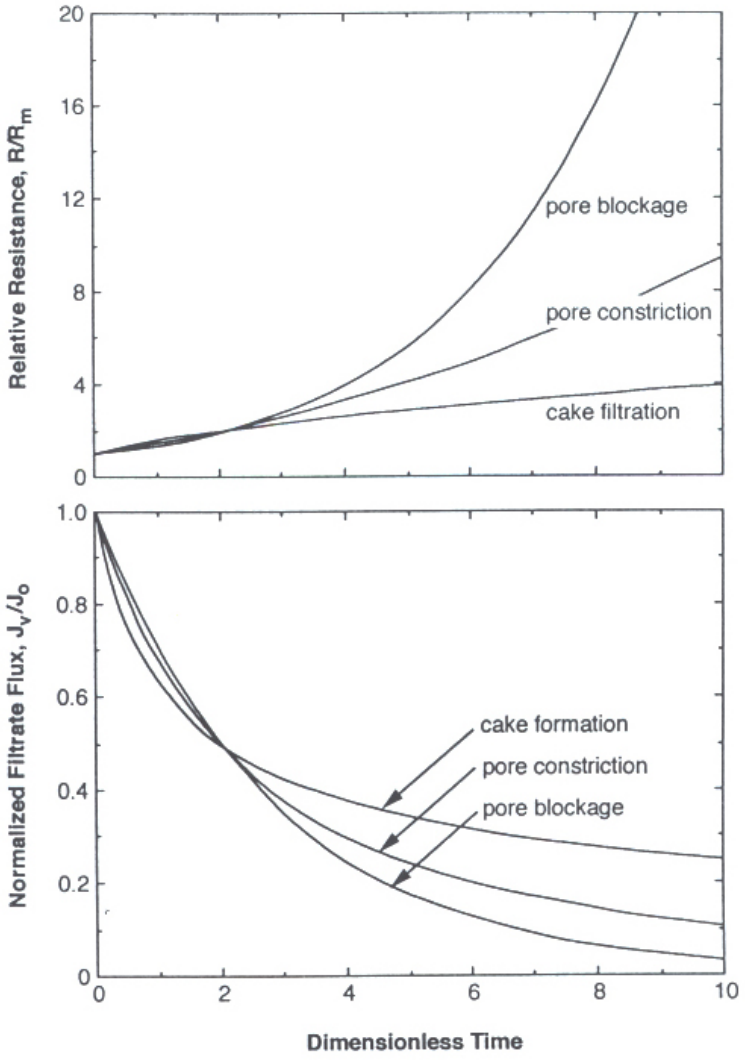

Figure 2 Comparison of pore blockage, pore constriction, and cake formation models. Upper panel shows the normalized resistance, lower panel shows normalized flux. [Zeman and Zydney, 1996]

In general, all three fouling mechanisms are simultaneously responsible for fouling of the ceramic membrane during particulate crossflow filtration. A model considering all the three fouling mechanisms, which was developed by Sondhi et al. [2000], agreed reasonably well with the experimental data. Working with a synthetic wastewater with a particle size distribution ranging from 1.5 to 10 μm and an average of 5 μm, the rate constant for the cake formation mechanism is 4-5 orders of magnitude larger than those for pore blocking and

constriction mechanisms for the 0.2 μm pore membrane, indicating cake formation is the dominating fouling mechanism; for the 0.8 μm pore membrane, the rate constant for the cake formation is 2-3 orders of magnitude larger than the other two, indicating an increased contribution of pore blocking and constriction mechanisms to the fouling; for the 5 μm membrane, the rate constant for pore blocking becomes 1 orders of magnitude larger than that for the cake formation, showing pore blocking is the dominant fouling mechanism in this case.

1.2.2 Theory for dead-end microfiltration

When the sieving mechanism of microfiltration is dominant, a cake layer of rejected particles usually forms on the membrane surface. The pressure-driven permeate flux through this cake layer and the membrane may be described by Darcy's law:

$$J \equiv \frac{1}{A}\frac{dV}{dt} = \frac{\Delta P}{\eta_0 (R_m + R_c)} \tag{8}$$

Knowledge regarding membrane and cake resistance is best gained from experimental measurements. Semi-empirical formulas, however, are available to estimate R_m and R_c [Ho and Sirkar, 1992].

1.2.2.1 Membrane resistance

Membrane resistance depends on the membrane thickness, nominal pore size, and various morphological features such as the tortuosity, porosity, and pore size distribution. For a membrane whose pores are assumed to consist of cylindrical capillaries of uniform radius

perpendicular to the face of the membrane, the resistance can be calculated by using the Hagen-Poiseuille equation:

$$J = \frac{n_p \pi r_p^{\,4} \Delta p_m}{8 \eta_0 L} \tag{9}$$

where n_p is the number of pores per unit area, L is the membrane thickness. Accordingly, R_m (unit: m^{-1}) is given by

$$R_m = \frac{\Delta p_m}{\eta_0 J} = \frac{8L}{n_p \pi r_p^{\,4}} \tag{10}$$

indicating that the membrane resistance increase with increasing membrane thickness and decrease with increasing pore size and number density. It will also increase with time if fouling or particle capture in the membrane interior occurs.

Porosity (ε_m) is defined as the membrane void volume/total volume, and specific surface area (S_m) ≡ pore surface area/solids volume. For a membrane with uniform cylindrical pores, $\varepsilon_m = n_p \pi r_p^{\,2}$ and $S_m = 2\pi n_p r_p/(1 - \varepsilon_m)$, which can be derived from their definition directly. Using these parameters, Eq. (10) becomes

$$R_m = \frac{K(1-\varepsilon_m)^2 S_m^{\,2} L}{\varepsilon_m^{\,3}} \tag{11}$$

where K = 2 for membranes with uniform cylindrical pores. For membranes with other pore structure, Eq. 11 may still be used, but with the value of the constant K varying with the membrane morphology and pore structures [Ho and Sirkar, 1992].

1.2.2.2 Cake resistance

When a cake is incompressible, its porosity and resistance are independent of the imposed pressure drop. The cake resistance is then often estimated by the Carman-Kozeny equation, which is of the same form as Eq. 11:

$$R_c = \frac{K(1-\varepsilon_c)^2 S_c^{\,2} \delta_c}{\varepsilon_c^{\,3}} \tag{12}$$

where δ_c is the cake thickness, ε_c is the void fraction of the cake, and S_c is the solids surface area per unit volume of solids in the cake. For rigid spherical particles of radius r, the specific surface area is $S_c = 3/r$, the void fraction ε_c of a randomly packed cake is approximate 0.4, and the constant K is reported by Grace [1953] to be 5.

Noting that the cake resistance is proportional to its thickness, a specific cake resistance per unit thickness is defined as

$$\hat{\alpha} \equiv R_c / \delta_c \tag{13}$$

Often, cake permeability K_c is reported instead, where $K_c = \hat{\alpha}^{-1}$. An alternative quantity is the specific cake resistance on a mass basis (unit: m/kg)

$$\alpha \equiv R_c / w \tag{14}$$

where w is the mass of cake deposited per unit area of membrane. These quantities can be related as follows;

$$w = \rho_s (1-\varepsilon_c)\delta_c \tag{15}$$

$$\hat{\alpha} = \rho_s (1-\varepsilon_c)\alpha \tag{16}$$

where ρ_s is the mass density of the solids comprising the cake.

Many cake materials, such as microbial cells, are highly compressible. Compressible cakes exhibit a decrease in void volume and an increase in the specific resistance as the compressive pressure is increased [Ho and Sirkar, 1992].

Specific cake resistance (α) is a function of particle diameter (d_p), porosity of cake (ε), and particle density (ρ). A well established empirical relationship for α is Carman's equation [Carman, 1938]:

$$\alpha = 180(1-\varepsilon)/(\rho \cdot d_p{}^2 \cdot \varepsilon^3) \qquad \text{(unit: m/kg)} \tag{17}$$

The smaller floc size, the greater cake resistance.

For compressible or deformable particles, specific surface is difficult to evaluate. Thus Darcy's law can be used in the form [Ward, 1987]

$$J = \frac{1}{A}\frac{dV}{dt} = \frac{\Delta P}{\mu\alpha(1-\varepsilon)\rho_s\delta_c} \tag{18}$$

1.2.3 Cake compressibility

The effect of cake compressibility can be estimated by assuming that the specific cake resistance is a power law function of the imposed pressure drop:

$$\alpha = \alpha_0 \Delta P^n \tag{19}$$

where α_0 is a constant related primarily to the size and shape of the particles forming the cake, n is the cake compressibility index, which varies from zero for an incompressible cake to a value near or even exceeding unity for a highly compressible cake. These quantities are estimated by measuring the specific cake resistance at various pressure drops, for example,

ranging between 0.5 - 2.0 bar [Borelage et al., 2003], and then plotting the logarithm of α versus the logarithm of Δp.

Constant pressure filtration using a dead-end cell system under unstirred condition (not to disturb the C_b in feed water) can be used to test α [Kang, et al. 2003; Lee et al. 2001; Ho and Sirkar, 1992]. Plotting t/V vs. V, knowing other parameters, α can be calculated as follows [Boerlage, et al., 2003, 1998; Nakanishi, et al., 1987]:

$$\frac{t}{V} = \frac{\mu R_m}{A\Delta P} + \frac{\mu C_b \alpha}{2A^2 \Delta P} V \tag{20}$$

Derivation of Eq. 20 is given in the appendix A. Typically this plot shows three regions corresponding to blocking, cake filtration and cake compression (Figure 3). The first sharp increase in slope is attributed to blocking, followed by cake filtration which is a linear region of minimum slope. Modified fouling index (MFI) is defined as the slope of this line.

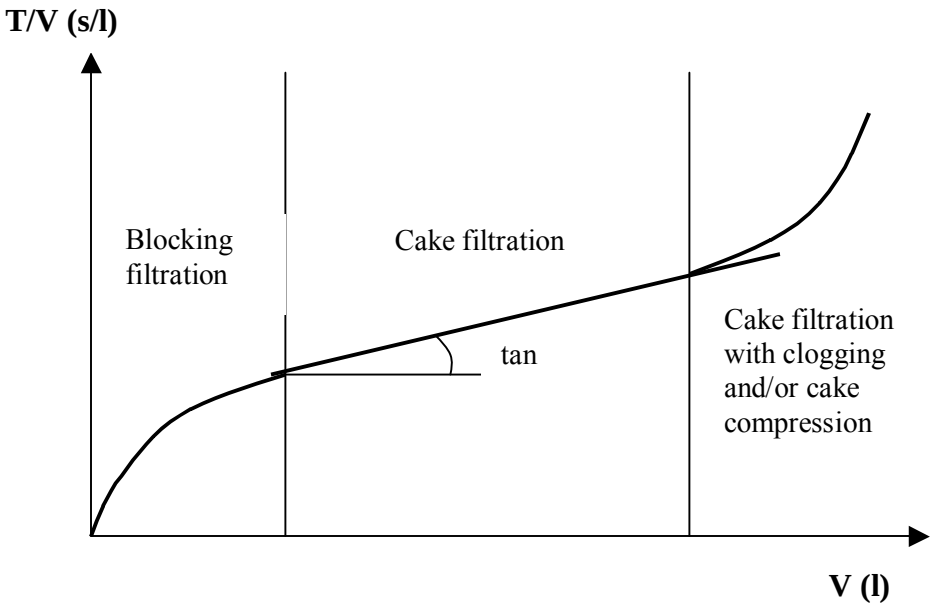

Figure 3 Ratio of filtration time (t) and filtrate volume (V) as a function of filtrate volume (V). MFI determined from the gradient slope of the linear portion of the t/V vs. V plot [Boerlage, et al., 2003].

The specific cake resistance also can be calculated according to Eq. 21 using the slope of the plot of $1/J^2$ vs. t. This equation is derived from Darcy's law and the derivation was given by Chudacek and Fane [1984].

$$\frac{1}{J^2} = (\frac{R_m \mu}{\Delta P})^2 + \frac{2\mu C_b \alpha}{\Delta P} t \qquad (21)$$

Although useful in practice, Eq. 19 represents an oversimplification of the behavior of compressible filter cakes. For example, it assumes that the cake compression depends on the pressure drop across both the membrane and the cake layer rather than that of just the cake. Also, the porosity and specific cake resistance vary throughout the cake height [Ho and Sirkar, 1992], that is, α_x is a function of local porosity ε_x [Ward, 1987]. More explanation can be found in the segment 1.2.4 (Eq. 22, etc.).

1.2.4 Properties of compressible cake

A filter cake can be considered as a series of thin slices of thickness d*x* and porosity ε_x with their boundaries parallel to the membrane. The total pressure P applied onto the cake can give rise to two pressures within the cake, hydraulic pressure P_x and compressive drag pressure in the solids P_s, so that $P = P_x + P_s$, and $dP_x + dP_s = 0$. The hydraulic pressure P_x drops throughout the cake as the liquid flows frictionally through the particles. The drag force impacted to the particles causes compaction of the cake. The total drag force imparted from one particle to another at contact point divided by the cross-sectional area is termed compressive drag pressure P_s. It has been observed that ε_x is the lowest in the region close to the membrane where the hydraulic pressure P_x is low, and greatest at the interface between cake and suspension where P_x is high [Tiller and Kwon, 1998; Ward, 1987; Tiller and Green, 1973].

The relationship between porosity and pressure can be established experimentally by using a compression-permeability cell – a device in which the cake is consolidated under a mechanical loading of P_s, achieved by placing suitable weights on a porous solid plug positioned over the cake. The permeability as a function of resistance is then determined by allowing the filtrate to pass through the cake under a low hydrostatic head. In this apparatus, the permeability of the cake is determined and assumed to be equal to that of a filter cake where the apparent compressive pressure, $P_s = P - P_x$, is the same as the consolidation pressure used in the cell. The results of work using the above technique shows that in general

$$\alpha_X = \alpha_0 P_s^{\,n} \tag{22}$$

$$\varepsilon_X = \varepsilon_0 P_s^{\,-\lambda} \tag{23}$$

for P_s values greater than a minimum P_i, which is about 1.0 psi, where α_0 is the initial filtration resistance and ε_0 the initial porosity [Ward, 1987].

Several authors have developed approximate equations to predict the distribution of porosity within a cake. For example,

$$\frac{P_s}{P} = \left(\frac{1-x}{L}\right)^{1/(1-n-\beta)} \quad \text{for } P_s > P_i \tag{24}$$

where x is distance from membrane surface, β is the exponent in the relation

$$1 - \varepsilon_X = BP_s^{\beta} \tag{25}$$

B being a constant that varies from 0 to 0.25 [Ward, 1987].

For highly compressible beds of fragile flocs or biosolids derived from municipal wastewater, pressures exceeding some low value (generally less than 1 atm) neither increase the filtrate flow rate nor decrease the average cake solidosity (volume fraction of solids, solidosity + porosity = 1). [Tiller and Kwon, 1998].

1.2.5 Dynamic simulation/analysis of cake properties

A dynamic analysis is proposed by Hwang and Hsueh [2003] to estimate the cake properties during soft colloid microfiltration. The Tiller empirical equations [Tiller, et al. 1980] were used to relate the local cake properties in this analysis, two of which have been shown above as Eq. 22 and 25, another one is

$$1 - \frac{x}{\delta_c} = \frac{P_s^{1-n-\beta} - (n+\beta)^{1-n-\beta}}{\Delta p^{1-n-\beta} - (n+\beta)^{1-n-\beta}} \tag{26}$$

where *x* is the distance from the membrane surface. The results show that the entire filtration course can be divided into three stages. At the beginning, the deposition and rearrangement of the colloidal particles on the membrane surface cause the overall filtration resistance to increase. In the second stage, a rapid increase in filtration resistance and a decrease in cake porosity due to cake compression and colloid deformation can be found. A compact skin layer begins to be formed next to filter membrane in this stage. The skin thickness is about 10-20% of the entire cake thickness but this layer exhibits about 90% of the overall filtration resistance. The average cake porosity increases gradually in the third stage due to loose packing in the newly formed cake. The trend can be reflected in the dt/dV vs. V filtration curve, which is concave first then convex as shown in Figure 4, indicating a different shape from Figure 3 [Boerlage, et al. 2003, 1998]. The physical characteristics of a filter cake formed by soft colloids include:

1. highly deformable, the cake porosity depends strongly on the applied compressive pressure;
2. the retardation effect of cake compression, i.e. the equilibrium state cannot be instantaneously attained;
3. area contact between soft colloids;
4. Kozeny equation can no longer be used. Since porosity as low as 0.1 – 0.2 is frequently found in a filter cake formed by soft colloids, the Kozeny equation cannot be applied to relate the applied pressure and the flow rate of a fluid under this condition.

A viscoelastic model may be used to express the instantaneous variation of cake porosity during cake compression:

$$\frac{\varepsilon_t - \varepsilon_i}{\varepsilon_f - \varepsilon_i} = 1 - \exp(\frac{-t}{\tau}) \tag{27}$$

where ε_i is the local cake porosity before compression (t = 0), ε_f is the local cake porosity at equilibrium after compression ($t \to \infty$), ε_t is the local cake porosity at time t, and τ is the retardation time, which can be determined from the curves plotted using the cake porosity vs. time [Hwang and Hsueh, 2003; Lu, et al., 2001].

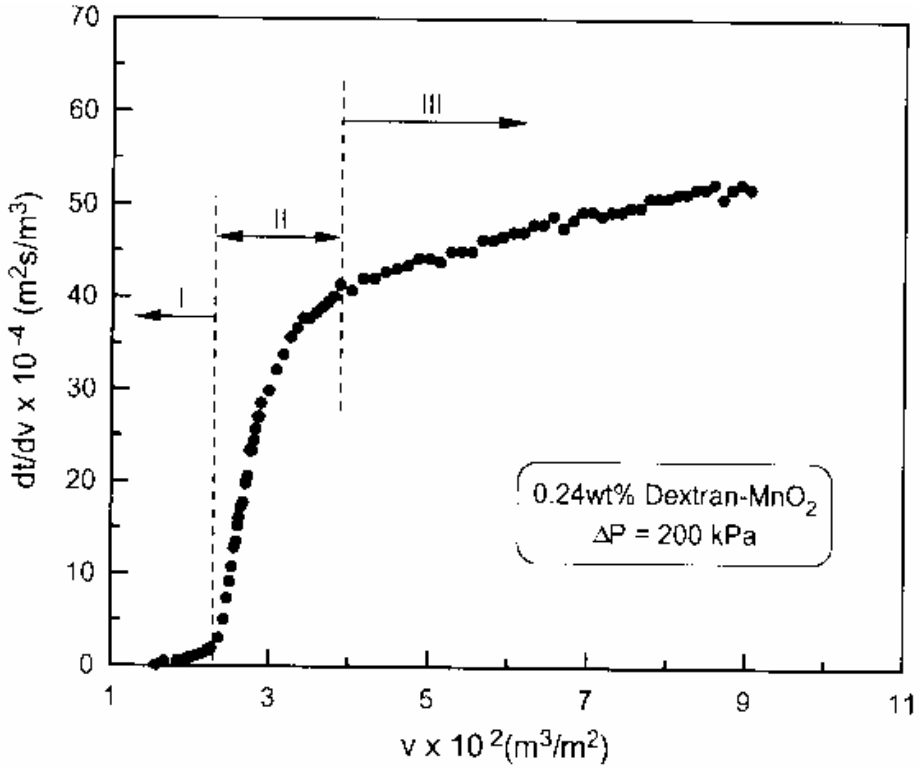

Figure 4 Filtration curve of dt/dV vs. V for Dextran-MnO_2 colloids under Δp = 200 kPa, where I, II and III stands for stage I (particle deposition), II (cake compression) and III (loose packing of newly formed cake) respectively. [Hwang and Hsueh, 2003]

1.2.6 Experimental method to measure cake porosity and thickness

A permeation experiment set-up consisting of a column at the base of which a membrane was inserted was used by Benkahla, et al. [1995] to determine the variation of porosity and thickness of the cake with pressure. The pressure over a previously deposited cake and the corresponding DI water flow rate were continuously measured with a data acquisition system. Ergun's equation was used as follows:

$$\Delta p = \frac{150}{(\phi d_p)^2}\frac{(1-\varepsilon)^2}{\varepsilon^3}\mu J \delta_c \tag{28}$$

where ϕ is the volumetric shape factor. The thickness is expressed with the known mass, m, of the previously deposited cake:

$$\delta_c = \frac{m}{\rho_s (1-\varepsilon) A} \tag{29}$$

Then,

$$\Delta p = \frac{150}{(\phi d_p)^2}\frac{(1-\varepsilon)^2}{\varepsilon^3}\mu J \frac{m}{\rho_s A} \tag{30}$$

Using Δp and J measured during a permeation experiment, this equation is solved by the Newton-Raphson method for the determination of ε.

The cake porosity also can be measured using thermal gravity analysis, i.e. measuring the wet to dry mass ratio [Hwang and Hsueh, 2003]. An optical in situ technique by reflection-type photointerrupter was adopted to measure the dynamic cake thickness [Lu et al., 2001]

1.3 SPECIFIC CAKE RESISTANCE OF ACTIVATED SLUDGE

The specific cake resistance of activated sludge is mainly affected by the presence of bacterial exocellular polymers including polysaccharides, proteins and lipids. Low dissolved oxygen (DO) level inhibited the self-flocculating abilities of bacteria and produced smaller sized flocs. As the particle size got smaller and dispersed solids concentration increased, the passage ways of water through the cake and filter medium during filtration was clogged, the resistance to the flow of water increased, so the specific resistance to filtration increased. At higher DO (2-5 mg/l), floc sizes were larger so that dispersed solids concentration was low. Flocs arrange themselves so as to leave large pores that would offer little resistance to flow during filtration. Gulas et al. [1979] also concluded "when activated sludge is well flocculated biologically, the time needed for filtration and therefore the specific resistance decreases appreciably." Water contained within well- formed flocs was floc water, which can be removed easily, so it resulted in a lower specific resistance. However, water inside dispersed sludge, like the particles in effluent, was capillary water. Removal of capillary water is independent of the applied vacuum or pressure. The increase of specific resistance of sludge from 10^{11} m/kg when DO was 5 mg/l (i.e. flocculated sludge) to 10^{15} m/kg when DO dropped to below 1 mg/l (i.e. dispersed sludge) could be explained by the above theory [Surucu and Cetin, 1989].

1.4 CRITICAL FLUX

Field et al. [1995] first introduced the concept of critical flux. The critical flux hypothesis for MF is that on start-up there exists a flux below which flux decline with time does not occur; above which fouling is observed. Recent studies have confirmed the existence of critical permeation flux in crossflow microfiltration [Gesan-Guiziou, et al., 1999]. Critical flux is tested under constant permeate flux condition and it indicates the flux below which TMP rises moderately and then can stabilize, but above which rapid rise in TMP will be observed. Limiting flux is tested under fixed TMP condition and means the flux when it becomes TMP independent, in other words, flux will not increase with increasing TMP above this limiting flux. Defrance and Jaffrin [1999] claimed that the critical and limiting fluxes were very close under the same conditions.

Arnot et al. [2000] examined three flux decline models and found the model developed by Field [1995] was the best to fit the experimental data. Its general equation is

$$dJ/dt = -k_J (J-J^*) J^{2-n} \quad (31)$$

where n depends on the fouling mechanism and J^* is the steady state flux. This approach to the analysis of flux data has the ability to identify the dominant mechanism, which has been shown to depend upon the membrane used and the operating conditions. n = 2.0 for complete pore blocking, n = 0 for cake filtration while n = 1 for intermediate mechanism. He also reported that the initial rate of fouling (dJ/dt at t = 0) during dead-end operation was proportional to Δp^3. For cross-flow operation, the initial rate of fouling increases with Δp.

1.5 EXPERIMENTAL METHOD TO DIFFERENTIATE HYDRAULIC RESISTANCES

Ousman and Bennasar [1995] and Jiraratananon and Chanachai [1996] designed a four-step experimental method for the determination of various hydraulic resistances including R_m, R_e (external fouling resistance, deposit), R_i (internal fouling resistance), and R_p (polarization layer resistance), and their respective importance in the fouling of membranes. This four-step experiment consisted of i) filtering DI water through the clean membrane to determine R_m, ii) filtering a suspension to determine R_t, iii) filtering DI water after rinsing away the polarization layer to determine R_p, and iv) filtering DI water after cleaning the membrane surface using a brush following by ultrasonic wave treatment with DI water to determine R_e and R_i. The step iv, however, is only applicable to inorganic membrane. The surface of polymeric membrane will be damaged by mechanical cleaning.

The tendency for membrane fouling in a membrane-coupled activated sludge system, that is, membrane bioreactor, was analyzed using resistance in series (R_f, R_c, R_t) model by Chang et al. [1999] and it was found that the cake layer resistance (R_c) made up most of the total resistance (R_t), but the fouling resistance (R_f), which was defined as the irreversible resistance caused by pore plugging and/or solute adsorption onto the membrane surface and pores, was negligible. The key factors controlling the R_c were the shape and size of the activated sludge flocs and the porosity of the cake layer accumulated on the membrane surface.

1.6 FRACTIONATION OF FOULANTS IN NATURAL WATER

A pre-filtration, fractionation and fouling determination protocol was adopted by Howe and Clark [2002] to investigate the mechanism and components in natural waters that contribute to fouling in microfiltration and ultrafiltration. Regenerated cellulose (RC) membranes with nominal molecular weight cutoff (MWCO) of 3000, 10000, 30000 and 100000 Daltons (unit of atomic weight, for example, atomic weight of hydrogen (H) is one Dalton) were used to fractionate the glass fiber filter permeate because RC exhibits low protein binding characteristics and is unlikely to retain material by adsorption or mechanisms other than size exclusion. Then, 0.2 μm polypropylene membrane was used to determine the fouling of each aliquot. Particulate matter (larger than 0.45 μm) was relatively unimportant in fouling as compared to dissolved matter. Very small colloids, ranging from 3000 – 100,000 Da, i.e. about 3 – 20 nm in diameter, appeared to be important membrane foulants. When the colloidal fraction was removed, the remaining dissolved organic matter (DOM), which was smaller than 3 nm and included about 85 – 90% of the total DOM, caused very little fouling. Adsorption was demonstrated to be an important mechanism for fouling by colloids.

1.7 FEASIBILITY OF USING MEMBRANE FILTRATION AS TERTIARY TREATMENT TECHNOLOGY

An analysis of MF performance with constant flux processing of secondary effluent was conducted by Parameshwaran, et al. [2001] and showed the filtrate of MF can be used without any further treatment for secondary purposes such as floor washing, etc. The MF unit was a hollow fiber module with gas backwash capability actuated when the TMP increased to 20 or

50 kPa. The difference between specific cake resistance α at 20 and 50 kPa were equivalent to a compressibility n of about 1.0.

Alonso et al. [2001] compared MF and UF consisted of prefiltration with two optional filtering thresholds of 400 and 30 μm in their application on filtration of secondary effluent of a conventional wastewater treatment plant, the results showed that both technologies produced the same quality output for the treated wastewater. It was only possible to observe some slight increase in the rates of color, phosphorus and nitrogen elimination for UF in relation to MF, but MF provided operational advantages over UF.

1.8 MICROFILTRATION/ULTRAFILTRATION OF PRIMARY OR SECONDARY EFFLUENTS

Bourgeous, et al. [2001] investigated the effects of feed water quality such as particle size distribution and concentration, mode of operation, and backwash effectiveness on UF performance. In the ultrafiltration of filtered (by passing through a granular medium filter) primary effluent (FPE), the severe flux decline and rapid fouling was imputed to pore blocking and/or constriction by the particles in the smaller size range, 0.4 – 5 μm, and they were difficult to be removed by typical backwash. Pre-filtration was proved useful and economical to maintain a better performance of UF. When processing both filtered and unfiltered secondary effluent, the UF system produced effluents equivalents to those of an oxidized, coagulated, clarified, and filtered wastewater as per Title 22 CWRC (State of California, 1978, 0 mg/l TSS, 1 mg/l BOD_5). Improved performance i.e. higher maintainable

flux with lower TMP and longer time between chemical cleanings was found by allowing flux to decline naturally, rather than using a constant flux mode of operation.

Treatment of primary effluent by coagulation with $FeCl_3$-adsorption by powder activated carbon (PAC)-ultrafiltration for reuse was explored by Abdessemed and Nezzal [2002]. A significant reduction of COD from 165 to 7 mg/l and 0 NTU turbidity effluent was achieved by this technique.

2.0 MATERIALS AND METHODS

2.1 EXPERIMENTAL SET UP

Figure 5 shows the dead-end stirred cell system used in this project. It consists of a nitrogen gas cylinder to provide constant trans-membrane pressure (TMP), a stainless steel feedwater reservoir whose capacity was about 2.5 liters, a dead-end stirred filtration cell with a capacity of around 350 ml, a beaker or a 5-liter plastic pail used as an effluent receiver and an electronic balance to measure the amount of effluent. The stirrer provides a high but undefined crossflow velocity, which facilitates reducing fouling on the membrane surface. A sinter metal plate provides support for the membranes.

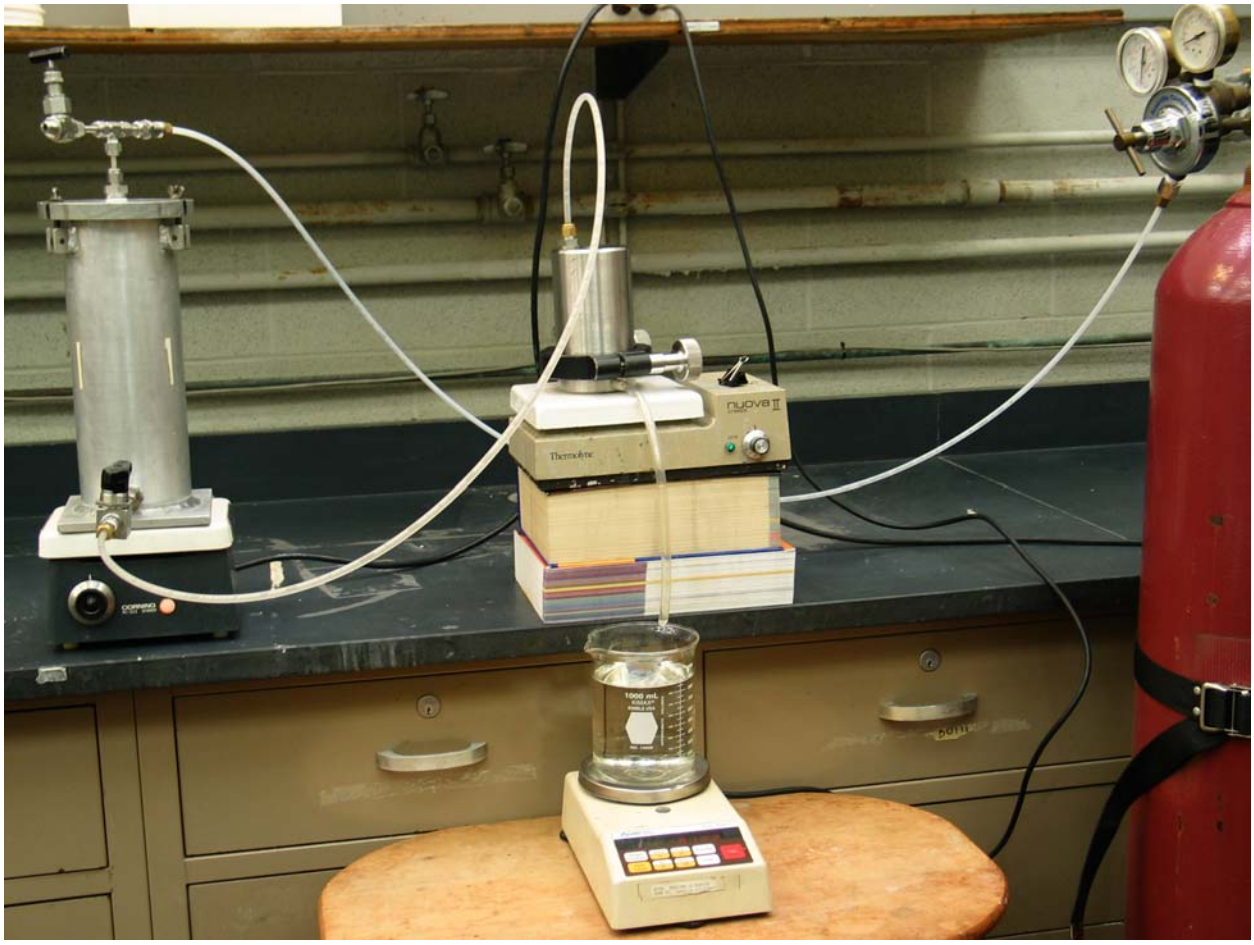

Figure 5 Experimental set up of the dead-end stirred cell system

2.2 FEEDWATER

The objective of this project is to explore the application of microfiltration as a tertiary treatment method for primary and secondary effluents from domestic wastewater treatment plants and the membrane fouling mechanism. Primary and secondary effluent from ALCOSAN Municipal Wastewater Treatment Plant in Pittsburgh, Pennsylvania were taken during the period of May to October 2003 and used for the laboratory research. Once the effluent samples in plastic carboy were brought back to lab, they were stored in 4^{o}C cold storage room and generally were not kept more than 2 weeks before being used for

experiment. When taking feedwater from the carboy, the carboy was shaken well to assure uniform composition.

Tap water in membrane lab, Benedum Engineering Hall, University of Pittsburgh was also tested to investigate whether this water could cause a similar or different type of fouling in microfiltration (MF).

2.3 WATER QUALITY ANALYSIS

Suspended solids (SS) and Volatile suspended solids (VSS) were measured for both primary / secondary effluents and tap water by following the protocol in Standard Methods [20th edition]. The values of suspended solids and turbidity were correlated by making a series of dilution of the freshly sampled primary effluent and measuring the two parameters respectively.

2.4 MEMBRANES

Flat sheet polymeric membranes were supplied by PALL Corporation. The technical specifications of Versapor®-200 w/wa ("w/wa" stands for with wetting agent) 0.2 μm (abbreviated as Versapor hereafter) and Supor®-200 0.2 μm (abbreviated as Supor hereafter) membranes are shown in Table 1. Versapor is naturally hydrophobic but is modified by the manufacturer to be hydrophilic. Thus, both membranes are hydrophilic but possibly Supor will stay hydrophilic for a longer amount of time with proper storage. Another advantage of

Supor is its higher porosity than that of Versapor [Personal communication with a technical consultant of PALL]. That is why its typical clean water flow rate is higher (Table 1).

Table 1 Technical specification of Versapor®-200 w/wa 0.2 μm and Supor®-200 0.2 μm membranes [Pall website]

Specifications	Versapor®-200 w/wa 0.2 μm	Supor®-200 0.2 μm
Filter media	Acrylic copolymer on a nonwoven support	Polyethersulfone, white
Typical water flow rate at 10 psi ($ml/min/cm^2$, ($m^3/m^2.s$))	16 (2.67E-3)	26 (4.33E-3)
Maximum operating temperature-water (^oC)	88	100
Minimum bubble point-water* (psi)	30	51
Sterilization	Non-sterile	Gamma irradiation

***** The bubble point is the pressure at which a steady stream of air bubbles emerges from the membrane. It is determined by wetting a membrane so that its pores are filled with liquid and applying air. The minimum air pressure required to displace the liquid from the pores is a measure of pore diameter and hydraulic resistance. The bubble point test is to ensure the integrity of a membrane by measuring the nominal size of the smallest pore.

2.5 DATA RECORDING AND PROCESSING

The flux of microfiltration with PALL membranes was investigated at a TMP of 15 psi. During filtration experiments the amount of filtrate and time elapsed were recorded manually with a stop watch. Steady state flux in this context is defined as the flux when it approximately attains a constant value.

2.6 FRACTIONATE MEMBRANE, CAKE AND IRREVERSIBLE RESISTANCES BY A 3-STEP TEST

A 3-step test with the stirred dead-end cell system under 15 psi and ~20 ^{o}C was designed to determine various hydraulic resistances: R_m (resistance of new membrane), R_c (deposited cake resistance) and R_i (irreversibly adsorbed layer, pore blocking and/or pore constriction, which can not be removed by washing), and their respective significance in the fouling of membranes. The membranes used in this experiment are Pall Versapor®-200W/Wa (acrylic copolymer) and Supor®-200 (polyethersulfone), both of which are hydrophilic 0.2 μm membranes without pre-coating. Deionized (DI) water with 17.8 megorm-cm resistivity produced in environmental lab, located in Benedum Engineering Hall of University of Pittsburgh, was used as clean water in step 1 and 3 of the 3-step test. The experimental procedure is as follows:

- Step 1 - DI water was filtered through the clean membrane, R_m can be calculated from Eq. 1,

$$R_m = \frac{\Delta P}{J_{v1} \times \eta_w} \quad (1)$$

- Step 2 - the feedwater was filtered until flux stabilizes, then R_t can be calculated from Eq. 2

$$R_t \equiv R_m + R_c + R_i = \frac{\Delta P}{J_{v2} \times \eta_w} \quad (2)$$

- Step 3 - the fouled membrane was washed using warm tap water (~38 ^{o}C) under a flow rate of about 1.9 m^3/m^2.s (1.5 GPM) for 10 min and then rinsed with DI water to remove the deposited cake layer. The washed membrane was tested with DI water again. $R_i + R_m$ can be calculated from Eq. 3

$$R_i + R_m = \frac{\Delta P}{J_{v3} \times \eta_w} \quad (3)$$

Therefore, $R_c = R_t - (R_i + R_m)$. All the permeate fluxes, i.e. J_{v1}, J_{v2} and J_{v3} here are stabilized flux rates measured when they do not change approximately over 1%.

2.7 SPECIFIC CAKE RESISTANCE (α) AND COMPRESSIBILITY INDEX N

Compressible cakes exhibit a decrease in void volume and an increase in the specific resistance as the compressive pressure is increased. The effects of cake compressibility can be estimated by assuming that the specific cake resistance is a power law function of the imposed pressure drop:

$$\alpha = \alpha_0 (\Delta p)^n \quad (4)$$

where α_0 is a constant related primarily to the size and shape of the particles forming the cake, and n is the cake compressibility, which varies from zero for an incompressible cake to a value equal or higher than unity for a highly compressibility cake [Ho and Sirkar, 1992]. The value of compressibility index n was estimated by measuring the specific cake resistance at various pressures, i.e. 10, 15, 20 psi using a dead-end cell system under unstirred condition in this study, and then plotting the logarithm of α versus the logarithm of Δp.

By plotting t/V vs. V of the filtration data, specific cake resistance (α) can be calculated according to

$$\frac{t}{V} = \frac{\mu \alpha C_b V}{2PA^2} + \frac{\mu R_m}{PA} \quad (5)$$

where t = accumulated time, V = accumulated volume of filtrate, A = filtration area, P = pressure, C_b = suspended solids concentration in the feed water, μ = viscosity of feedwater. This equation was originally used for vacuum filtration of sludge and derived from Darcy's law. It may be used for positive transmembrane pressure filtration as well. Thus,

$$slope = \frac{\mu C_b \alpha}{2A^2 \Delta P} \quad \text{(unit: s/m}^6\text{)} \tag{6}$$

then

$$\alpha = \frac{slope \times 2A^2 \Delta P}{\mu C_b} \quad \text{(unit: m/kg)} \tag{7}$$

There may be a convex or concave before the curve of t/V vs. V enters a linear phase. The slope of the linear phase will be taken for the calculation of α. Before filtering primary or secondary effluent, a new membrane was conditioned by filtering one cell capacity (~350 ml) of DI water. The tests under three different pressures were conducted using fresh sewage effluent samples whose storage time was within 24 hr. An amount of feed water enough for conducting the three tests was taken from the storage bucket and stored in another glass container, from which water sample was taken for SS measurement. The container was mixed well before taking water for each test to assure consistency of water quality. The value of SS was used as C_b in equation 7 for all the three runs.

2.8 COMPARISON AMONG DIFFERENT CLEANING METHODS IN STEP 3 OF THE 3-STEP TEST

Placing the efficiency of the selected cleaning method in comparison with more aggressive techniques, three alternative cleaning methods were tried and compared. They are respectively:

1. Hotter (53 ^{o}C) tap water at a higher flow rate of about 3.6 m^3/m^2.s (2.9 GPM) for 10 min;
2. Gentle scrubbing of the membrane surface with a toothbrush;
3. Gentle scraping of the membrane surface with a blade.

2.9 IRREVERSIBLE FOULING: A MULTI-CYCLE TEST OF PRIMARY EFFLUENT USING VERSAPOR MEMBRANE

After the optimum cleaning method was determined, filtration of primary effluent and membrane cleaning exactly like the second and third steps in the 3-step test were conducted repeatedly with a single sheet of Versapor membrane to investigate how the irreversible resistance would vary in a long-term operation, which simulated the actual field application. After each cycle, the membrane was soaked in DI water overnight at room temperature for next cycle test conducted in the next day. The primary effluent used in cycle 1-9 was from a same batch of sample, a second batch of water sample was taken for the following cycles. In addition, two controls were done at the same time using the same kind of membrane (new), one of which was to test whether soaking in DI water could influence the permeability of the membrane by measuring the membrane permeability after 1, 3 and 11 days of soak

respectively, the other was to test the influence of the cleaning method adopted in this experiment on the permeability of the membrane.

3.0 RESULTS AND DISCUSSION

The objective of this work focused on the understanding and quantification of microfiltration membrane fouling as applied to the management of primary and secondary sewage effluent from municipal wastewater treatment plants. A 3-step test was developed to fractionate the total hydraulic resistance into membrane, cake and irreversible fouling resistances and determine their individual contribution. This chapter will narrate in the sequence as follows:

- fractionation of hydraulic resistances in microfiltration for primary and secondary sewage effluent;
- determination of the specific cake resistance and compressibility index n of the particles in the sewage effluent;
- comparison between the fouling pattern of sewage effluent and tap water;
- optimization of the membrane surface cleaning methods to adjust the 3-step test procedure;
- a multi-cycle operation to investigate how the irreversible fouling varies in a long-term operation; and
- comparison between the data of sewage effluent microfiltration from this study and published data for sludge dewatering.

3.1 FRACTIONATE HYDRAULIC RESISTANCES

Total hydraulic resistance (R_t) of filtration consists of R_m (resistance of new membrane), R_c (deposited cake resistance) and R_i (resistances due to irreversibly adsorbed sticky foulants and pore blocking or constriction). To investigate their individual significances in microfiltration, the 3-step experimental method was developed to differentiate these three resistances using a stirred dead-end cell system. Briefly, the experimental procedure was as follows: Step 1: R_m was determined when deionized (DI) water was filtered through a clean membrane; Step 2: R_t was determined when the feed water was filtered until flux stabilized; and Step 3: the fouled membrane was washed using warm tap water (~38 ^oC) under moderate strength (about 1.9 $m^3/m^2.s$) for 10 min and then rinsed with DI water to remove the deposited cake layer, the DI water flux was again measured and $R_i + R_m$ was calculated. Thus, R_i and R_c could be calculated separately. The temperature of all the feed water and DI water filtered was ~ 20^oC. R_c in this context is defined as resistance caused by the deposited cake layer, which is removable by the cleaning method adopted. R_i is defined as the resistance which cannot be removed by the cleaning method.

3.1.1 Microfiltration of primary effluent

Two membranes from Pall, i.e. Versapor (acrylic copolymer) and Supor (polyethersulfone) were used in the dead-end microfiltration of primary effluent. Samples were collected at ALCOSAN WWTP during dry weather days and suspended solids (SS) values were in the range of 30-65 mg/l. Although the primary effluent used for the filtration tests with these two different membranes were not from the same batch of sample, it did not influence the final observation that cake layer resistance caused by primary effluent was around 70% of total

hydraulic resistance, indicating it was the dominating fouling mechanism (Table 2 and Figure 6). Comparing these two membranes, Supor showed a somewhat lower membrane resistance, i.e. higher clean water flowrate, which was in accordance with their technical specifications provided by the manufacturer (Table 1). As shown in Figure 7, the clean water flux (7-a) of Supor was higher than that of Versapor. The initial flux of Supor in step 2 was 1.08E-3 $m^3/m^2.s$ while that of Versapor was only 1.86E-4 $m^3/m^2.s$ (7-b), and Supor maintained a slightly higher flux than Versapor through the filtration. Although the clean water flux at steady state of Supor®-200 in step 3 was close to that of Versapor membrane, its initial flux was also much higher (7-c). The flux decline in step 3 for Supor membrane was likely due to that the whole dead-end cell system was not cleaned and rinsed with DI water thoroughly between step 2 and 3. The flux in step 3 should be basically stable if ultrapure water with a resistivity of 18.2 megorm-cm is used and the whole system is well cleaned and rinsed.

Table 2 Summary of hydraulic resistances and their respective significance in filtration of primary effluent using Versapor and Supor membrane

Membrane	Step	Stabilized flux, J_v ($m^3/m^2.s$)	Hydraulic resistance (m^{-1})		Contribution to the R_t (%)
Versapor	1	1.42E-03	R_m	7.27E+10	0.28%
	2	4.01E-06	R_t	2.58E+13	-
	3	1.46E-05	R_c	1.87E+13	72.6%
			R_i	7.00E+12	27.1%
Supor	1	2.13E-03	R_m	4.85E+10	0.21%
	2	4.57E-06	R_t	2.26E+13	-
	3	1.41E-05	R_c	1.53E+13	67.7%
			R_i	7.27E+12	32.2%

Note:

1. R_c – cake resistance, R_i – irreversible resistance, R_m – membrane resistance, R_t – total resistance
2. 3-Step test: I. Clean water filtration; II. Feed water filtration; III. Clean water filtration after membrane cleaning.
3. A sample calculation of the resistances was given in appendix B.

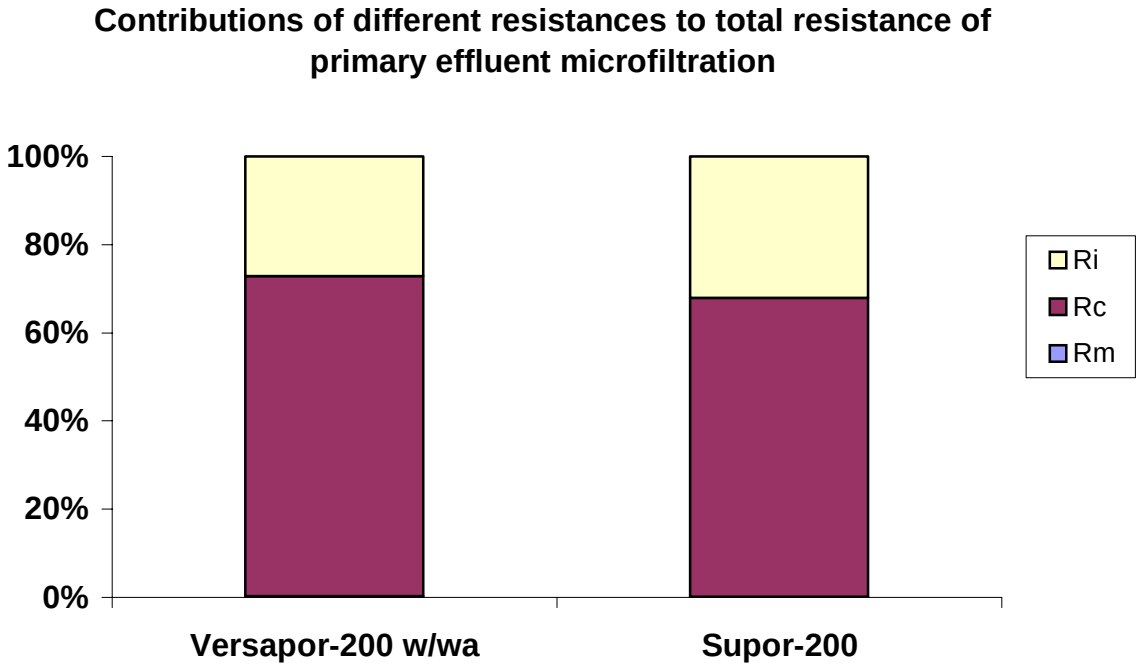

Figure 6 Fractionation of hydraulic resistances in filtration of primary effluent. R_c – cake resistance, R_i – irreversible resistance, R_m – membrane resistance.

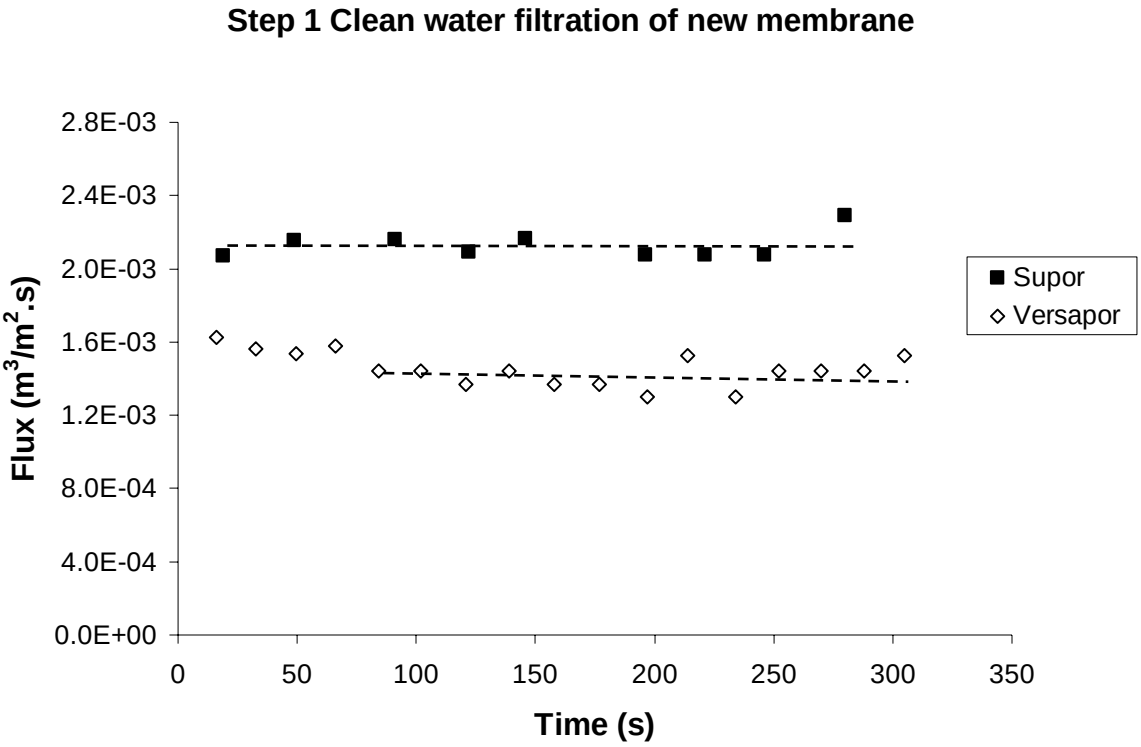
Step 1 Clean water filtration of new membrane
2.8E-03
2.4E-03
2.0E-03
1.6E-03
1.2E-03
8.0E-04
4.0E-04
0.0E+00
Flux (m3/m2.s)
0
50
100
150
200
250
300
350
Time (s)
Supor
Versapor

7-a

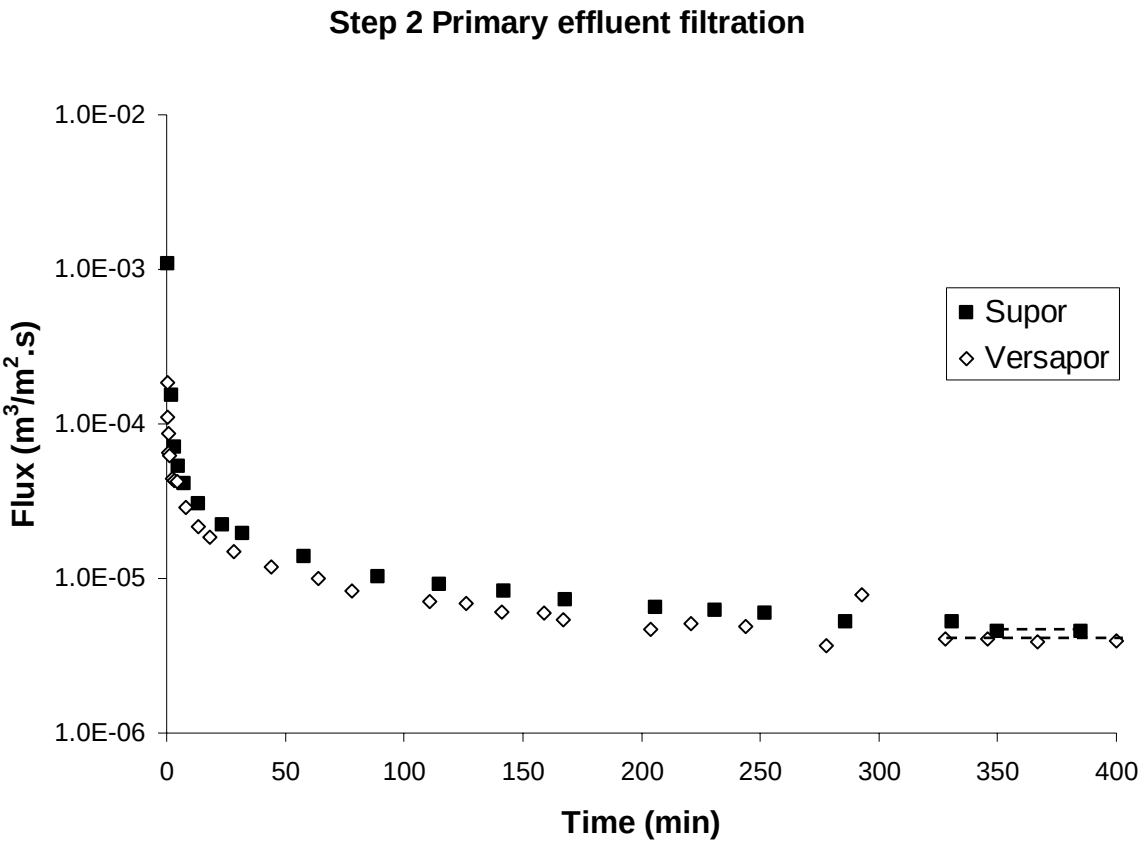
Step 2 Primary effluent filtration
1.0E-02
1.0E-03
1.0E-04
1.0E-05
1.0E-06
Flux (m3/m2.s)
0
50
100
150
200
250
300
350
400
Time (min)
Supor
Versapor

7-b

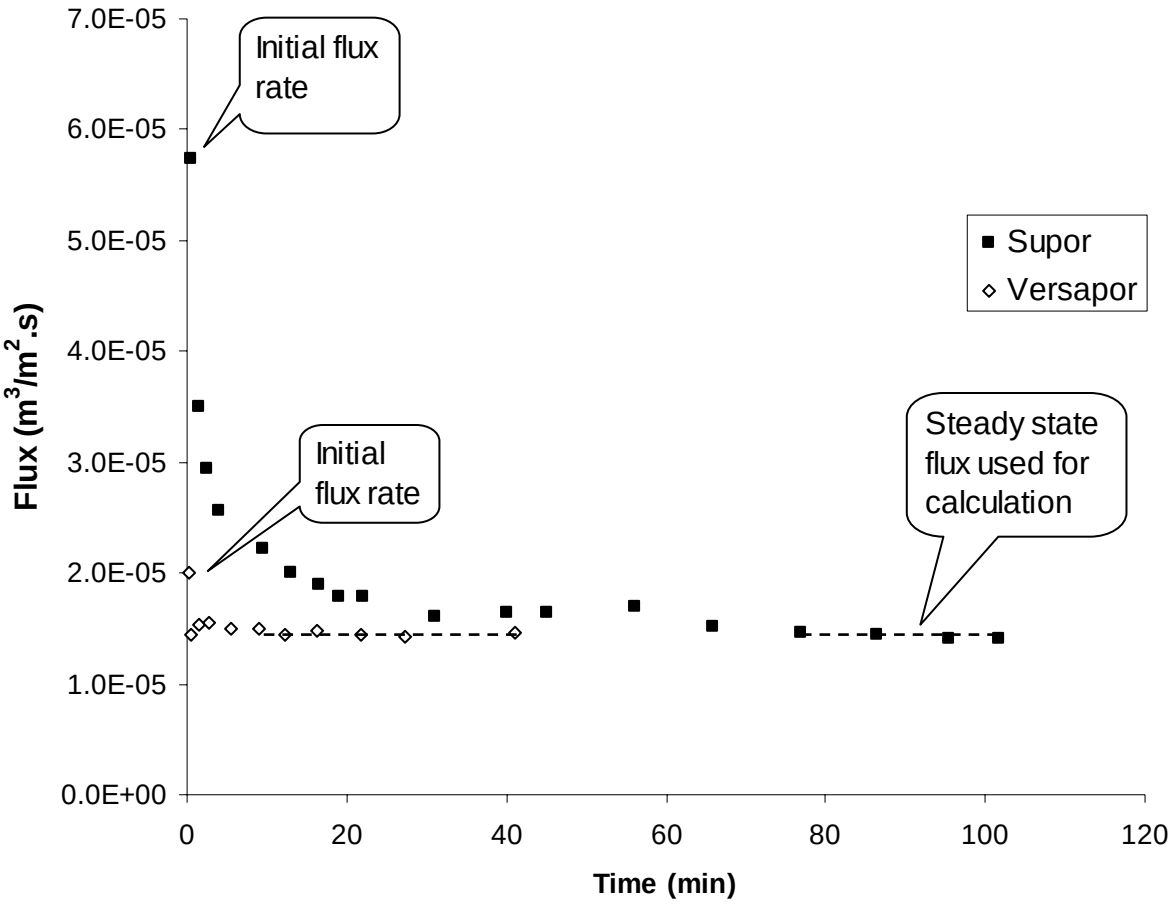

7-c

Figure 7 Comparison of the flux rates of primary effluent filtration by the 3-step test (I. clean water filtration; II. feed water filtration; III. clean water filtration after membrane surface cleaning) under 15 psi, stirred condition using Versapor membrane and Supor membrane. The dotted line showed how the steady state fluxes were determined.

3.1.2 Microfiltration of secondary effluent

Two different batches secondary effluent, one of which was sampled in a wet weather day (SS $\approx$2 mg/l), and another in a dry weather day (SS $\approx$8 mg/l), were tested with Supor membranes. Further, the two membranes, Supor and Versapor, were compared for their application in secondary effluent filtration. The same batch of secondary effluent was used for this comparison.

3.1.2.1 Filtration of secondary effluent sampled in a wet vs. dry weather day

As shown in Table 3-b, c and Figure 8, removable cake resistance (R_c) in the secondary effluent filtration contributed more to the total hydraulic resistance, which was up to 83-87% R_t. There was not significant difference between secondary effluent taken from a dry and wet weather day in terms of values of R_m, R_c, and R_i as well as their respective significance to the total hydraulic resistance.

Table 3 Summary of hydraulic resistances and their respective significance for (a) dry weather secondary effluent using Versapor membrane, (b) wet weather and (c) dry weather secondary effluent using Supor membrane

Membrane	Sample	Step	Stabilized flux, J_v ($m^3/m^2.s$)	Hydraulic resistance (m^{-1})		Contribution to the R_t (%)
Versapor	a. Dry weather	1	1.65E-03	R_m	6.26E+10	0.7%
		2	1.09E-05	R_t	9.47E+12	-
		3	6.65E-05	R_c	7.92E+12	83.6%
				R_i	1.49E+12	15.7%
Supor	b. Wet weather	1	2.01E-03	R_m	5.14E+10	0.6%
		2	1.13E-05	R_t	9.13E+12	-
		3	8.55E-05	R_c	7.92E+12	86.7%
				R_i	1.16E+12	12.7%
	c. Dry weather	1	2.13E-03	R_m	4.85E+10	0.5%
		2	1.00E-05	R_t	1.03E+13	-
		3	5.92E-05	R_c	8.56E+12	83.1%
				R_i	1.69E+12	16.4%

Note:

R_c – cake resistance, R_i – irreversible resistance, R_m – membrane resistance, R_t – total resistance;

3-Step test: I. Clean water filtration; II. Feed water filtration; III. Clean water filtration after membrane cleaning.

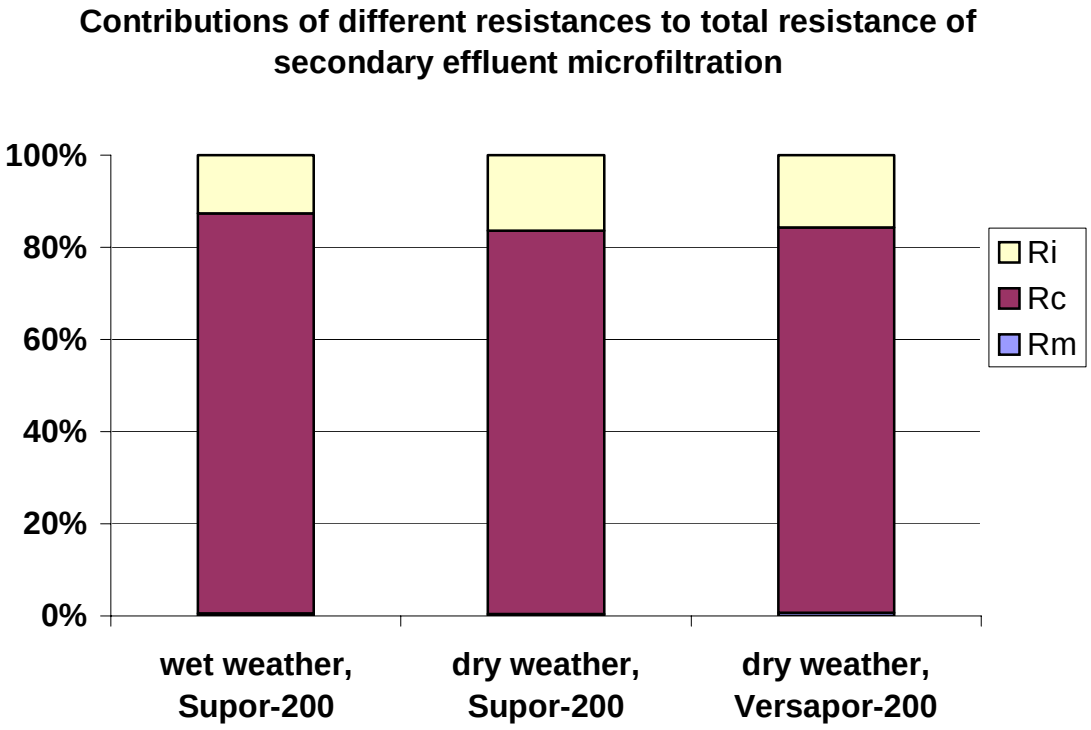

Figure 8 Fractionation of hydraulic resistances in filtration of secondary effluent taken in a wet weather day and a dry weather day. R_c – cake resistance, R_i – irreversible resistance, R_m – membrane resistance.

3.1.2.2 Comparison between Supor and Versapor in secondary effluent filtration

Table 3- a & c and figure 8 also show the two membranes exhibited very similar cake and irreversible resistances and relative contribution to the total resistance, nonetheless, as shown in Figure 9, the productivity (volume of filtrate collected after certain period of time) of Supor was higher than that of Versapor. The fluxes of these two membranes in step 2 were compared in Figure 10. It could be seen that Supor membrane maintained a slightly higher flux rate at the starting stage of step 2, i.e. around first 20 minutes, after that, it became very close to that of Versapor membrane. Combining the results of primary effluent filtration shown in Figure 7 where Supor membrane remained somewhat higher flux rates throughout the filtration process, it may be deemed that Supor membrane performed marginally better in sewage effluent filtration than Versapor membrane in terms of flux rate and productivity.

To sum up, cake resistance (R_c) was the dominating fouling mechanism for both primary (~70% of R_t) and secondary effluent (~84% of R_t) microfiltration. Supor membrane showed a slightly better performance than Versapor membrane in filtering sewage effluent.

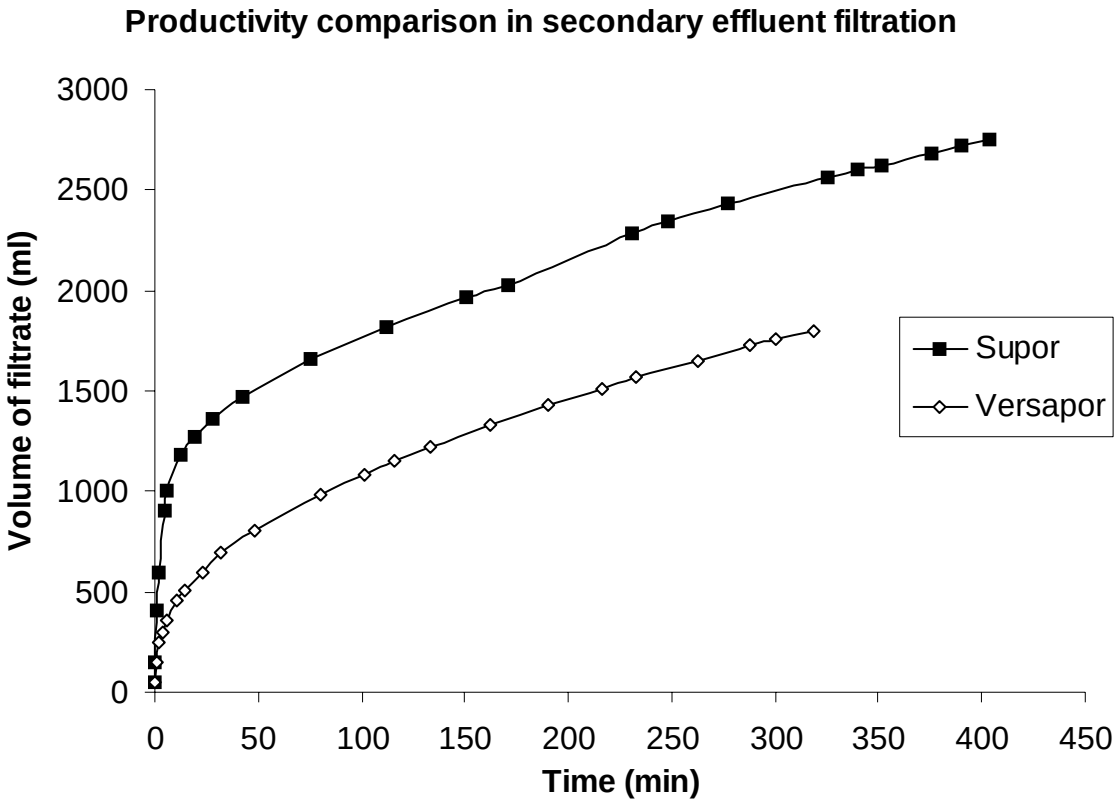

Figure 9 Productivities of Versapor and Supor membrane in filtration of secondary effluent taken in dry weather day under15 psi

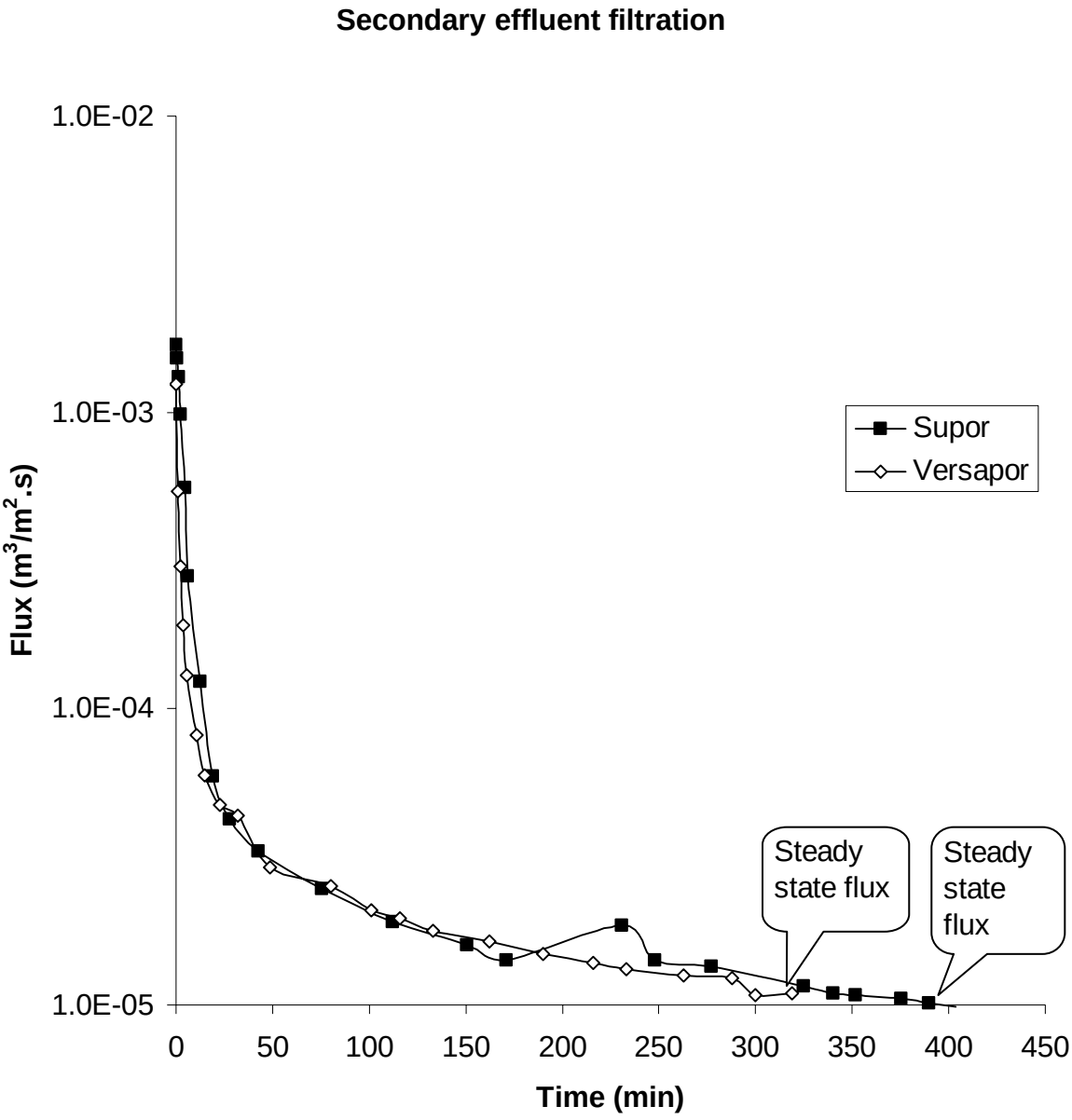

Figure 10 Flux rates of Versapor and Supor membrane in filtration of secondary effluent taken in dry weather day under15 psi

3.2 SPECIFIC CAKE RESISTANCE (α) AND COMPRESSIBILITY INDEX N

This section measures compressibility index, an indicator of whether the particles in the primary and secondary effluent are compressible or deformable. If they are compressible, any formulas only applicable to incompressible cake such as Carman-Kozeny equation may not be suitable in dealing with cake resistance (R_c) of microfiltration of primary/secondary effluents.

Since the specific cake resistance can be assumed to be a power law function of the imposed pressure drop, that is, $\alpha = \alpha_0 (\Delta p)^n$, the compressibility n can be known by measuring the specific cake resistance at various pressure drops and then plotting the logarithm of α versus the logarithm of Δp [Ho and Sirkar, 1992]. Plotting t/V vs. V of the filtration data, specific cake resistance (α) can be calculated according to $\frac{t}{V} = \frac{\mu \alpha C_b V}{2PA^2} + \frac{\mu R_m}{PA}$. For comparison purpose, Table 4 shows reported compressibility indices of selected microorganisms, particles, and activated sludge.

Table 4 Compressibility indices of selected microorganisms and particles [Nakanishi, et al. 1987]

Items	Compressibility index, n
B. circulans	1.0
R. spheriodes	0.88
Activated sludge	0.4-0.85 [Vesilind, 1974]
E. coli	0.79
Baker's yeast	0.45
M. glutamicus	0.31
Sand	0.0

Primary effluent

This series of filtration tests for studying the compressibility of the particles in primary effluent was conducted with Versapor membranes. The primary effluent sample was collected in a dry weather day and its suspended solids value was 64 mg/l. A comparison between the SS concentrations of the sewage effluent samples and the corresponding daily and monthly average SS data provided by the analytical lab of Alcosan was given in Table 5. This comparison verified the sewage effluent samples taken for this project were basically representative. The discrepancy between own analytical results and the Alcosan daily data resulted from that the former was from a grab sample but the latter was from a 24-hour composite sample.

As shown in Figure 11, the plots of t/V vs. V were linear almost from very beginning except for the first few seconds. Thus, slopes were measured by only considering the linear phase of each curve. Table 6 shows that the higher the pressure applied, the smaller the slope,

indicating the permeate flux increases with increasing TMP within the range of 10-20 psi. Figure 13 shows the compressibility index n of the primary effluent was 0.56, indicating the suspended solids were moderately compressible since "n=0" represents incompressible and "n=1" represents highly compressible cake.

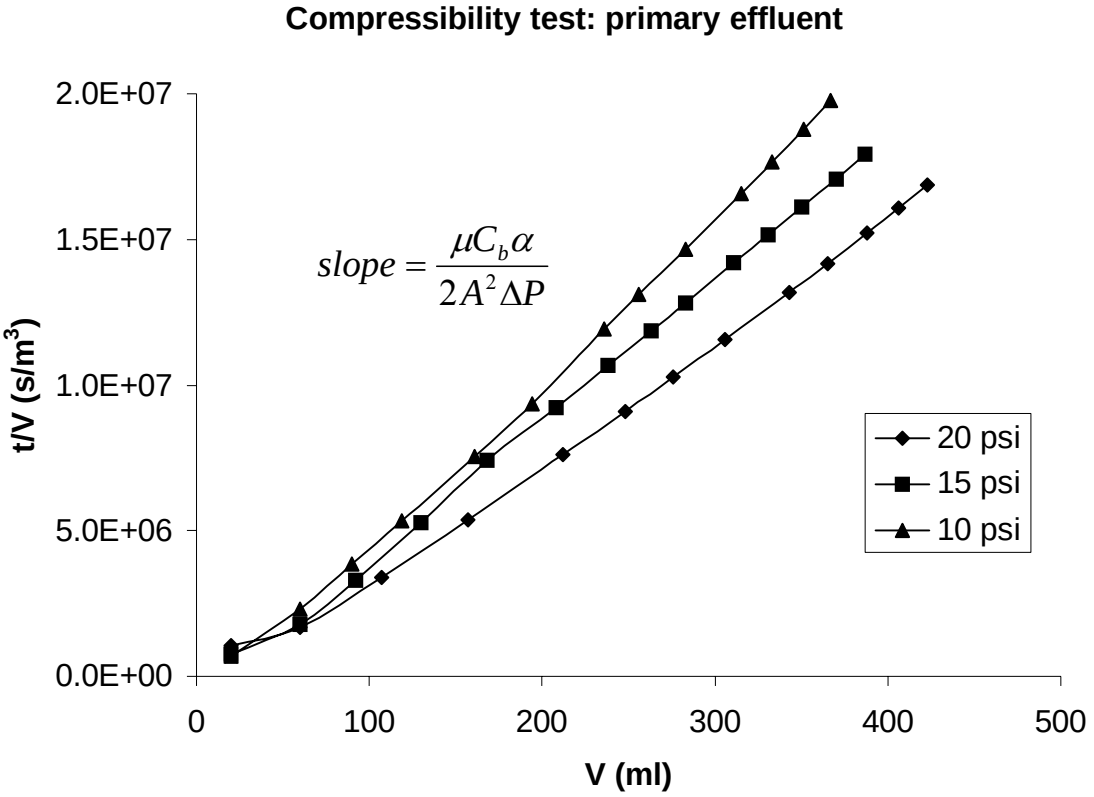

Figure 11 Summary of plots of t/V vs. V for primary effluent filtrations under different pressures, C_b = 64 mg/l.

Table 5 Comparison between the suspended solids concentrations of the sewage effluent samples and the corresponding daily and monthly average SS data provided by the analytical lab of Alcosan

Samples	Sampling Date	Own Analytical Results (mg/l)	Corresponding Alcosan Daily Data (mg/l)	Corresponding Alcosan Monthly Average Data (mean ± standard deviation) (mg/l)
Primary Effluent	8/11/2003	50	66	70 ± 27
	9/18/2003	64	52	52 ± 16
Secondary Effluent	10/9/2003	11	8	10 ± 2.1

Table 6 Specific cake resistance (α) values under different pressures for primary effluent

P (psi)	P (Pa)	Slope ($*10^{10}$)	α (10^{15} m/kg)
10	68948	5.721	1.82
15	103422	4.928	2.36
20	137896	4.211	2.68

Note: a sample calculation of α was given in appendix C

3.2.2 Secondary effluent

The same experiments were repeated for secondary effluent taken in a dry weather day with a suspended solids value of 11 mg/l. The plots of t/V vs. V for secondary effluent (Figure 12) showed a different shape from those of primary effluent. Before the linear phase, there was a gentle increasing phase and concave, which could become much more obvious for secondary effluent taken in a wet weather day, i.e. a lower SS level (figure was not shown). In other words, the more diluted the secondary effluent, the longer the gentle increasing phase before its linear phase. This looks like the shape of first 2 stages of the 3-stage filtration curve for compressible Dextran-MnO_2 colloids under $\Delta p = 200$ kPa shown in Figure 4 [Hwang and Hsueh, 2003]. The difference is the latter has a convex phase following the linear phase, i.e. the third stage. The reason why the filtration curve of secondary effluent did not show the third stage may be that the amount of particles in the effluent filtered in this study was relatively small so that the cake formation was still in the stage 2, i.e. skin layer phase. Nonetheless, the consistence of the filtration curve of secondary effluent to the first two stages of the typical curve for compressible particles indicated the particles in the effluent were compressible.

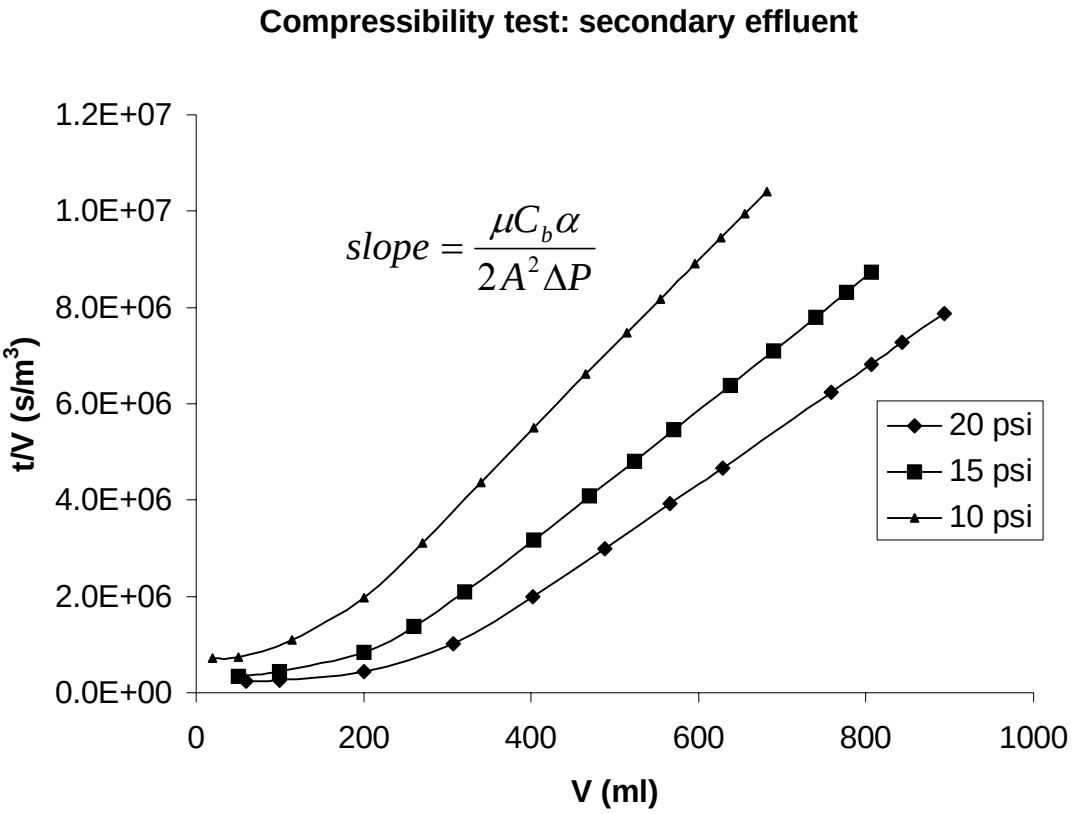

Figure 12 Summary of plots of t/V vs. V in secondary effluent filtration, C_b = 11 mg/l.

Table 7 Specific cake resistance α values under different pressures for secondary effluent

P (psi)	Pa	Slope ($*10^{10}$)	α (10^{15} m/kg)
10	68948	1.768	3.28
15	103422	1.379	3.84
20	137896	1.208	4.48

Note: a sample calculation of α was given in appendix D

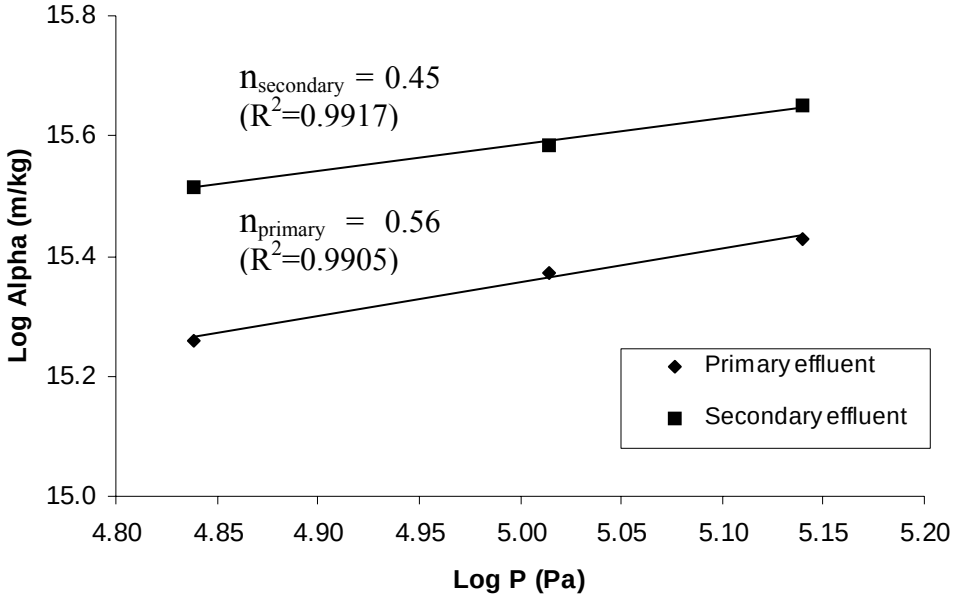

Figure 13 Plotting log α vs. log P to get compressibility index n of particles in sewage effluent according to $\alpha = \alpha_0 (\Delta p)^n$

Compressibility index for domestic wastewater sludge was found to range between 0.4 – 0.85 [Vesilind, 1974]. In a study of microfiltration of secondary effluent with constant flux processing conducted by Parameshwaran, et al. [2001], the compressibility index n of particles in the secondary effluent was reported to be about 1.0. As shown in Figure 11, in this study, the compressibility index n of solids in secondary effluent was 0.45, which was about the same as that of primary effluent. It might be concluded that the suspended solids in the secondary effluent has similar compressibility to those in primary effluent.

VSS can be approximately used as a measure for the biomass in the water and these microorganisms are compressible particles. Therefore, it might be hypothesized that higher proportion of VSS of the SS in the sewage effluent will result in higher compressibility index

of the particles. If the activated sludge tanks work very well, the well-flocculated sludge can aggregate more microorganisms so that the concentration of dispersed microorganisms in the effluent would be low. Therefore, the compressibility index n of particles in secondary effluent may fluctuate a little bit depending upon the operation condition of activated sludge tanks and clarifiers.

From Table 6 and 7, we can find the specific cake resistance (α) of particles in secondary effluent was around double that of particles in primary effluent. This finding accords with the statement in literature that primary sludge has lower α than secondary sludge.

3.3 FILTRATION OF TAP WATER AND DI WATER

Municipal water is the basic matrix of domestic wastewater. Taking into account that clean tap water has minimal level of microorganism and low turbidity, a different fouling mechanism may be expected.

DI water was used as clean water in this study to evaluate clean membrane flux rates. The DI water used in this study, whose resistivity was 17.8 megorm-cm, was run for a longer time, i.e. a larger amount, to see whether the DI water has any impurities to result in flux decline.

3.3.1 Tap water filtration

The objective of this section is to investigate whether the fouling mechanism of municipal tap water was similar to those of primary and secondary effluents. Two preliminary filtration runs were done with Supor membranes (Figure 14). The first run, the tap water filled during

the period of 11 - 26 min had visual light brownish color, which resulted from contamination from local distribution system, while the tap water was clear throughout the second run. Nonetheless, deep brown and red dense cakes were formed in both runs. The color of the cake of the second run was slightly lighter than that of the first run. A possible iron contamination in the tap water used in the first run may be the reason. The color and appearance of the cake caused by tap water was totally different from that caused by primary and secondary effluents.

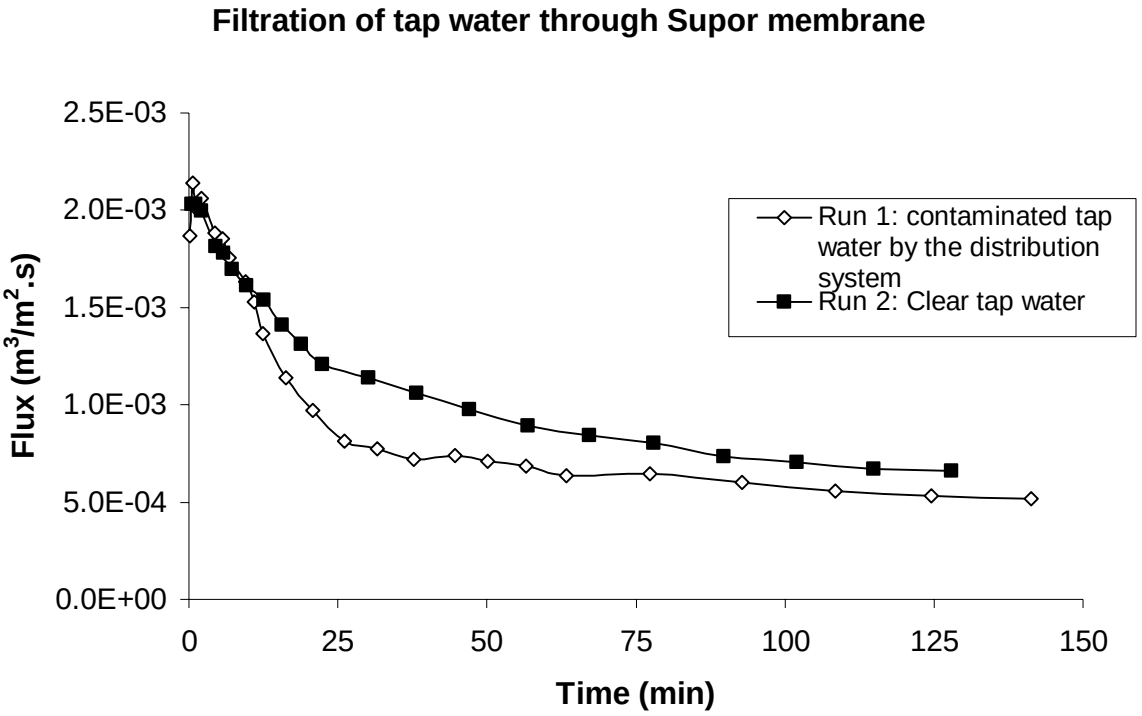

Figure 14 Flux decline of tap water in the filtration using Supor membrane

The 3-step test introduced in section 2.6 in chapter 2 was further conducted for visually clear tap water. The flux rates of the step 2 – tap water filtration of and the step 3 – DI water filtration after membrane surface cleaning were shown in Figure 15. The deep brown and red

dense cake formed in step 2 could not be removed by the warm and gentle water flushing method, suggesting that the resistance was "irreversible". This R_i occupied up to 73.7% of the total resistance R_t, while removable cake resistance (R_c) was comparatively small, only 3.3% of the R_t. This is summarized in Table 8. Obviously, this fouling mechanism was totally different from those of sewage effluent (Figure 16). The much lower proportion of VSS in SS for tap water (Table 9) indicated a different component and character of particles in the tap water from those in sewage effluent and resulted in this different fouling pattern.

The significant difference of fouling pattern between sewage effluent and tap water, and the fact that proportion of cake resistance (R_c) to the total hydraulic resistance in secondary effluent filtration is higher than that in primary effluent filtration suggest that the deposited cake properties and fouling mechanism are related to the characteristics of the particles in the feed water. It seems that cakes formed by inorganic particles are hard to remove, and cakes containing microbial flocs are relatively easy to be removed.

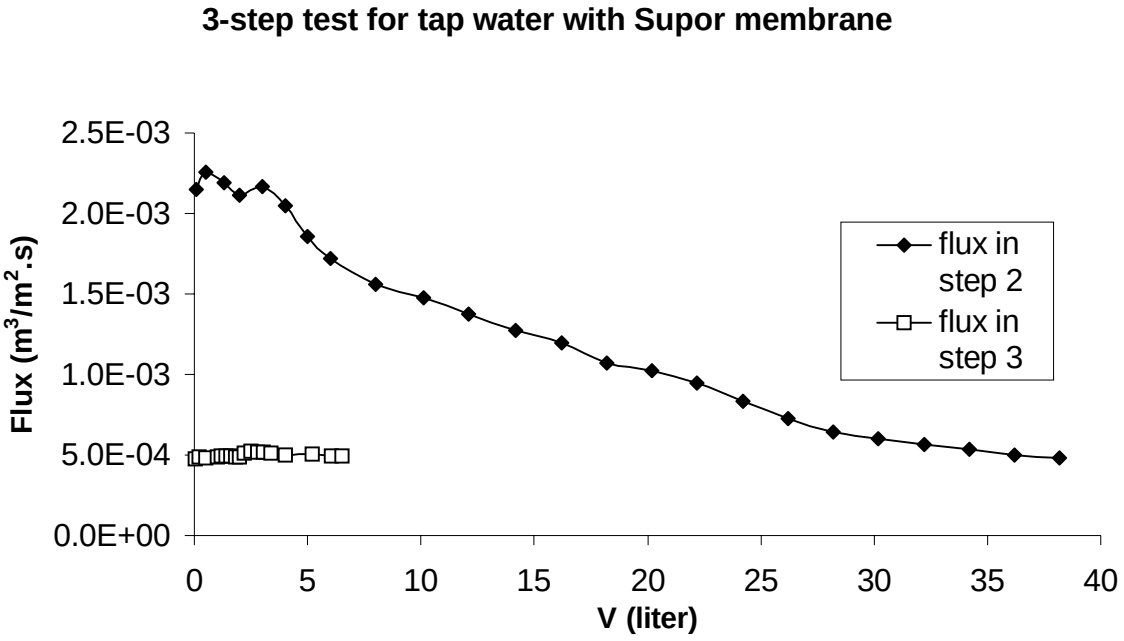

Figure 15 Variation in permeate flux of tap water in the step 2 and 3 of the 3-step test (I. DI water filtration; II. feed water filtration; III. DI water filtration after membrane surface cleaning by warm (~38^{o}C) and gentle water flushing (1.5 GPM)) with Supor membrane at 15 psi, flux in step 2 means tap water flux, flux in step 3 means clean water flux of the fouled membrane after cleaning

Table 8 Relative contribution to flux resistance for tap water filtration with Supor membrane

Step	Stabilized flux, J_v ($m^3/m^2.s$)	Hydraulic resistance (m^{-1})		Contribution to the R_t (%)
1	2.10E-03	R_m	4.92E+10	23.0%
2	4.84E-04	R_t	2.13E+11	-
3	5.00E-04	R_c	0.07E+11	3.3%
		R_i	1.57E+11	73.7%

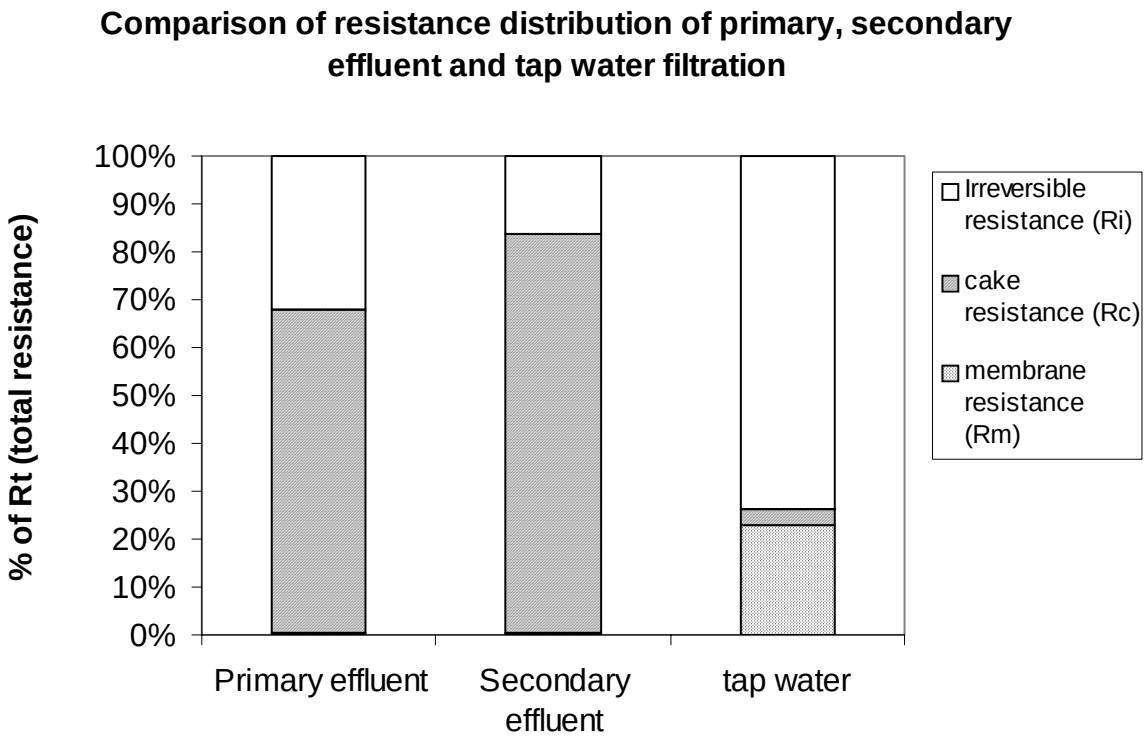

Figure 16 Comparison of the fouling mechanisms of primary/secondary effluents and tap water

Table 9 Suspended solids and volatile suspended solids in primary and secondary effluents, and tap water

	Primary effluent	Secondary effluent in a dry weather day	Secondary effluent after a wet weather day	Tap water
SS (mg/l)	34.3	7.6	2.3	0.475
FSS (mg/l)	8.6	1.6	0.43	0.375
VSS (%)	76.9	81.0	81.3	21.1

Note: 3 to 4 replicates were done for the measurements.

3.3.2 DI water filtration

The test for DI water filtration was run for around 2 hours, in the first 80 minutes of which about 38 liters of DI water was filtered. It was stopped since an approximately stable flux was reached. In the next 40 minutes of the 2 hours, to investigate whether membrane filtered DI water would result in smaller flux decline, the permeate collected in the first 80 minutes was filtered again as feed water. However, it turned out a similar slightly declining trend (Figure 17), which may suggest that the main foulants from the DI water used are those soluble substances. After the test, there were tiny particles deposited on the membrane and the filtration area became faint yellow. The particles could be removed by washing with water, leaving a seemingly clean surface but with very faint color, which might be caused by small particles or high molecular weight colloids inside the pores (pore blocking and pore constriction). It can be concluded the slight flux decline was caused by the impurities in the DI water. Supposing ultrapure water is used, a constant flux rate may be expected.

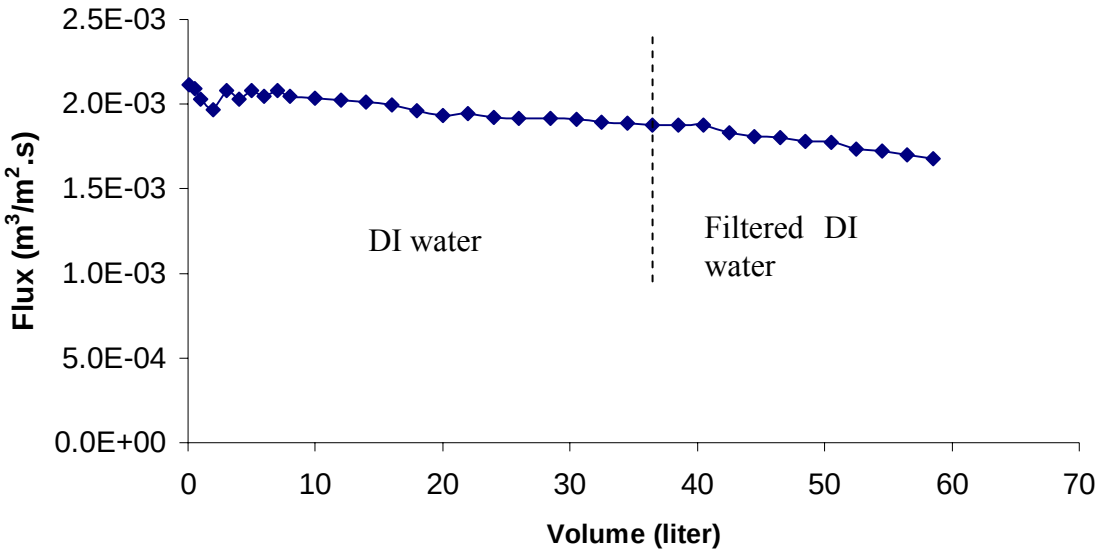

Figure 17 Flux declines of DI water (left part) and permeate, i.e. filtered DI water (right part) in the filtration using Supor membrane

3.4 COMPARE DIFFERENT CLEANING METHODS TO REMOVE CAKE RESISTANCE R_c

This section compared the other three membrane surface cleaning methods to investigate whether the cleaning method adopted in the step 3 of the 3-step test for removing the cake resistance, i.e. flushing the fouled membrane with warm tap water (~38 ^{o}C) at a flow rate about 1.5 GPM for 10 min, was sufficient to wash away all of the removable cake or not aggressive enough. The three more aggressive cleaning methods are hotter (53 ^{o}C) tap water at a higher flow rate of 2.9 GPM for 10 min, gentle scrubbing of the membrane surface with a toothbrush, and gentle scraping with a blade. Figure 18 shows the four methods respectively. Versapor membranes and primary effluents were used in this series of tests. It was observed that method 3 - gentle scrubbing with toothbrush and 4 - gentle scraping with blade were

more effective in removing the cake layer. As shown in Table 10, more aggressive cleaning resulted in better resistance removing effect. Method 2 - hotter (53 ^{o}C) and strong tap water (about 3.6 m^3/m^2.s, i.e. 2.9 GPM) flushing for 10 min, however, was only slightly less effective to reduce hydraulic resistance than method 3 and 4, but much better than method 1, i.e. the previously adopted method. Taking into account that physical abrasion with a toothbrush or a blade is not practical and may take a risk damaging the membrane itself, method 2 was finally chosen to be the optimum cleaning method applying to the 3-step test aiming at defining the different flux resistances. Therefore, the 3-step test was adjusted by adopting hotter and stronger tap water flushing as the cleaning method in the step 3 henceforth. That part of resistance that can be removed by this adjusted cleaning procedure was defined as deposited cake resistance while the resistance cannot by removed by this procedure as irreversible resistance hereafter in the study.

(a) Warm (38 ^{o}C) tap water flushing at a flow rate about 1.9 $m^3/m^2.s$

(b) Hotter (53 ^{o}C) tap water flushing at a flow rate about 3.6 $m^3/m^2.s$

(c) Gentle scrubbing with a toothbrush

(d) Gentle scraping with a blade

Figure 18 Comparison of four cleaning methods to be adopted in step 3 of the s-step test

Table 10 Influence of physical abrasion of membrane on restoring permeate flux

Cleaning methods	R_t (total resistance, m^{-1})	R_i (irreversible resistance, m^{-1})		R_c (cake resistance, m^{-1})	
		Value	% of R_t	Value	% of R_t
1. Warm (38 ^oC) and moderate tap water (about 1.9 $m^3/m^2.s$) flushing for 10 min	2.72E13	4.73E12	17.4	2.24E13	82.4
2. Hotter (53 ^oC) and strong tap water (about 3.6 $m^3/m^2.s$) flushing for 10 min	2.74E13	1.42E12	5.2	2.59E13	94.6
3. Gentle scrubbing with toothbrush	2.80E13	4.93E11	1.76	2.75E13	98.07
4. Gentle scraping with blade	2.80E13	8.13E11	2.9	2.71E13	96.9

Note: A complete version of this table is shown in Appendix E.

3.5 MULTI-CYCLE TEST OF PRIMARY EFFLUENT

The purpose of this multi-cycle test is to investigate how the magnitude of irreversible and cake resistance and their respective proportion to the total flux resistance will change with repeated cycles of filtration and cleaning. This simulates actual industrial practice of membrane processes. Filtration of primary effluent and membrane cleaning exactly like the second and third steps in the 3-step test were conducted repeatedly in this experiment and the irreversible resistance (R_i) in each cycle was determined, which was the so-called multi-cycle test. The adjusted membrane cleaning method - hotter (53 ^oC) and strong tap water (about 3.6 $m^3/m^2.s$) flushing for 10 min was adopted herein.

The primary effluent used for cycle 1-9 was from a single batch of sample, while a new batch of sample was taken for cycle 10-17. The initial SS of the second batch of primary effluent sample was 50 mg/l, equal to 34 NTU in turbidity. The correlation of SS and turbidity was shown in Figure 19. Because the measurement of turbidity is much faster than that of SS, the turbidity is measured for the stored sample to indicate whether its SS concentration varies over the storage period. A decrease of turbidity with storage time was observed although the sample was stored at 4 ^oC. For example, the turbidity was 27 NTU in day 8 and 24.5 NTU in day 11. With the assumption that the turbidity values can reflect the SS concentration, the latter turbidity value equaled to 34 mg/l in SS, meaning a 32% reduction. The possible reason might be due to lysis of the microorganisms during storage, or coagulation or clinging to wall of container. Therefore, a storage period less than 2 weeks was strongly recommended by the author. Nonetheless, the storage time for the primary effluent used for cycle 7-9 exceeded this time limit, which may be the reason resulting in the fluctuation of stabilized fluxes and

significance of irreversible resistance (R_i) in these three cycles (Table 11). Another sign indicating the effluent had been stored too long was that the color of the cake formed in the step 2 showed a darker color, but the usual color of the cake when the effluent filtered was still relatively fresh would be in between yellow and brownish. Based on this, the results of cycle 7-9 would be treated as erroneous points when plotting the trend line of R_i (Figure 20, 21).

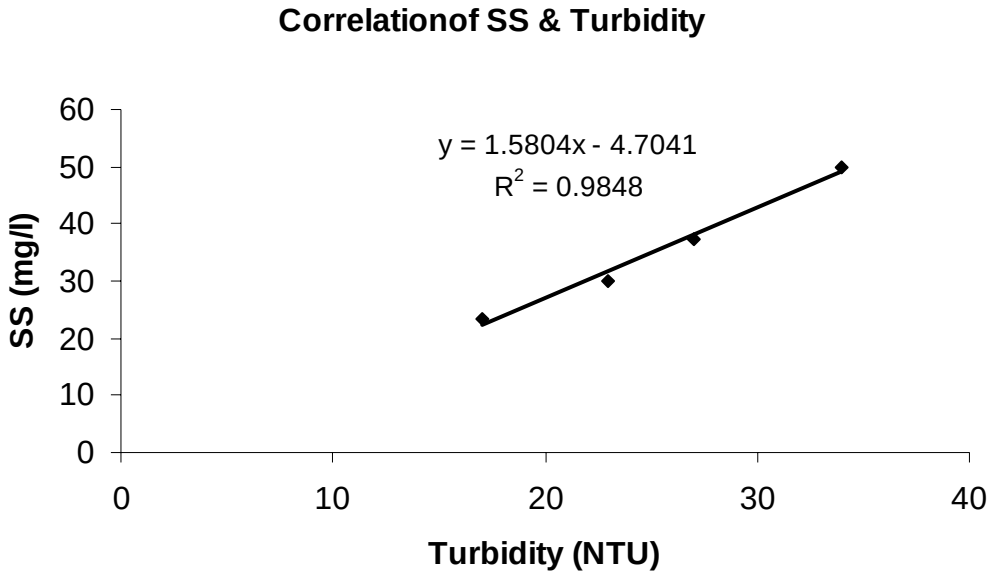

Figure 19 Correlation between suspended solids (SS) and turbidity of primary effluent

After each time of cleaning in the step 3, with the removal of deposited cake layer, a yellowish color left behind on the membrane, which may be caused by pore plugging and/or solute adsorption onto the membrane surface. At the end of 17 cycles testing with the same membrane, the color of the membrane deepened a little bit, becoming a color in between yellowish and lightly brownish.

Table 11 Summary of data of multi-cycle experiments

Cycle No.	Stabilized flux, J_v ($m^3/m^2.s$)		R_t (total resistance, m^{-1})	R_i (irreversible resistance, m^{-1})		R_c (cake resistance, m^{-1})	
	Step 2 (J_{v2})	Step 3 (J_{v3})		Value	% of R_t	Value	% of R_t
1	3.77E-06	7.02E-05	2.74E+13	1.42E+12	5.2	2.59E+13	94.5
2	3.63E-06	3.59E-05	2.84E+13	2.83E+12	10	2.55E+12	89.8
3	3.62E-06	2.92E-05	2.85E+13	3.48E+12	12.2	2.50E+13	87.7
4	3.87E-06	2.66E-05	2.67E+13	3.83E+12	14.3	2.28E+13	85.4
5	4.09E-06	2.55E-05	2.52E+13	4.00E+12	15.9	2.12E+13	83.9
6	4.16E-06	2.15E-05	2.48E+13	4.75E+12	19.2	2.00E+13	80.6
7	5.56E-06	2.13E-05	1.86E+13	4.80E+12	25.8	1.38E+13	74.2
8	5.24E-06	1.83E-05	1.97E+13	5.59E+12	28.4	1.41E+13	71.4
9	5.84E-06	2.70E-05	1.77E+13	3.77E+12	21.3	1.39E+13	78.5
10	3.45E-06	2.15E-05	2.99E+13	4.75E+12	15.9	2.51E+13	83.9
11	3.41E-06	1.96E-05	3.03E+13	5.22E+12	17.2	2.50E+13	82.6
12	3.92E-06	1.98E-05	2.63E+13	5.16E+12	19.6	2.11E+13	80.2
13	4.27E-06	1.98E-05	2.42E+13	5.16E+12	21.3	1.90E+13	78.5
14	4.26E-06	1.89E-05	2.42E+13	5.41E+12	22.4	1.87E+13	77.3
15	4.37E-06	2.03E-05	2.36E+13	5.03E+12	21.3	1.85E+13	78.4
16	4.60E-06	2.04E-05	2.24E+13	5.01E+12	22.4	1.73E+13	77.4
17	4.77E-06	2.35E-05	2.16E+13	4.34E+12	20.1	1.72E+13	79.6

Note: J_{v1} = 2.20E-3 $m^3/m^2.s$, R_m = 4.69E10 m^{-1}.
Step 2: primary effluent filtration; Step 3: clean water filtration after membrane surface cleaning

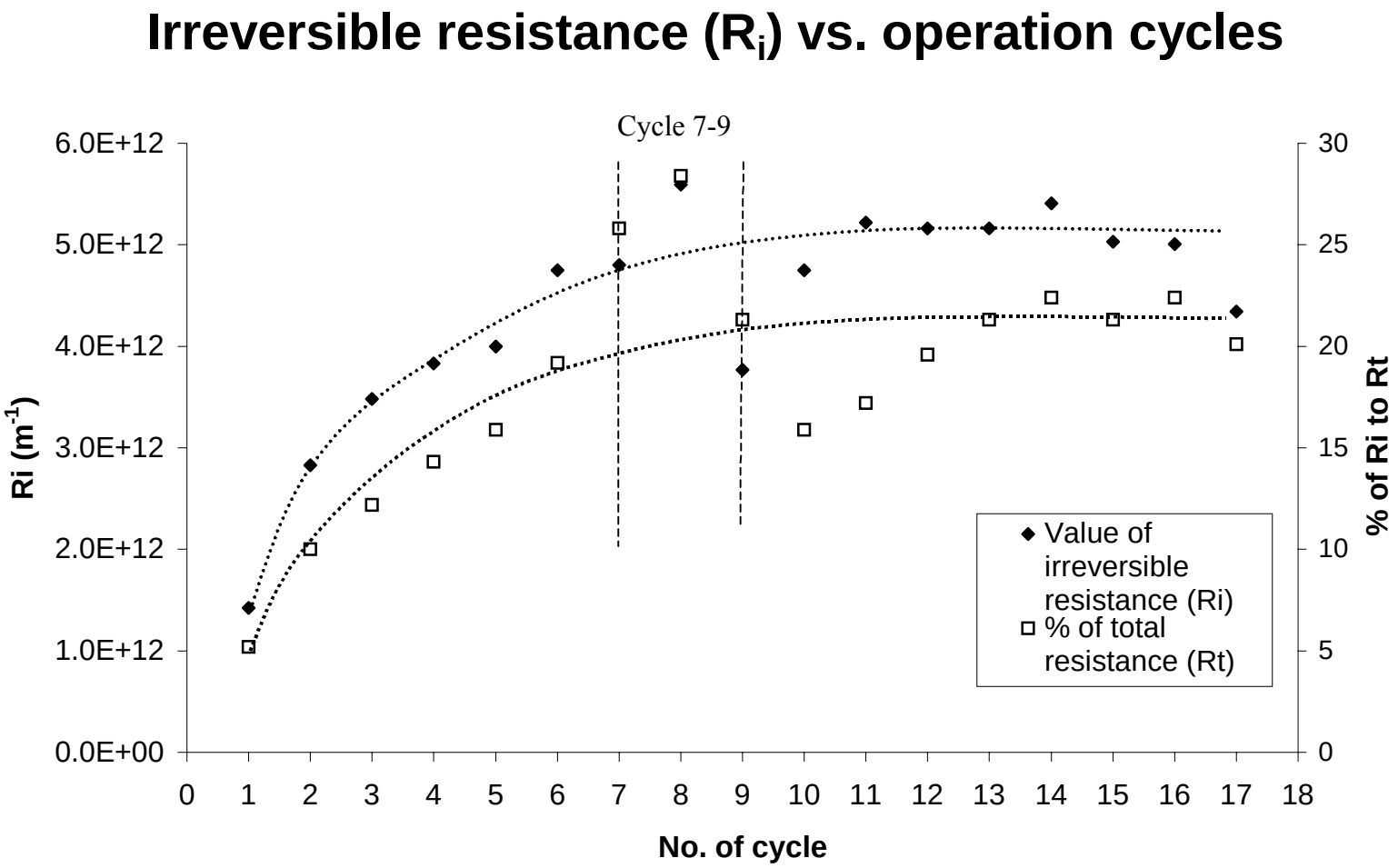

Figure 20 Comparison of irreversible resistance (R_i) and its fraction to total hydraulic resistance (R_t), i.e. R_i/R_t, in different cycles. The dotted line was added as trend lines.

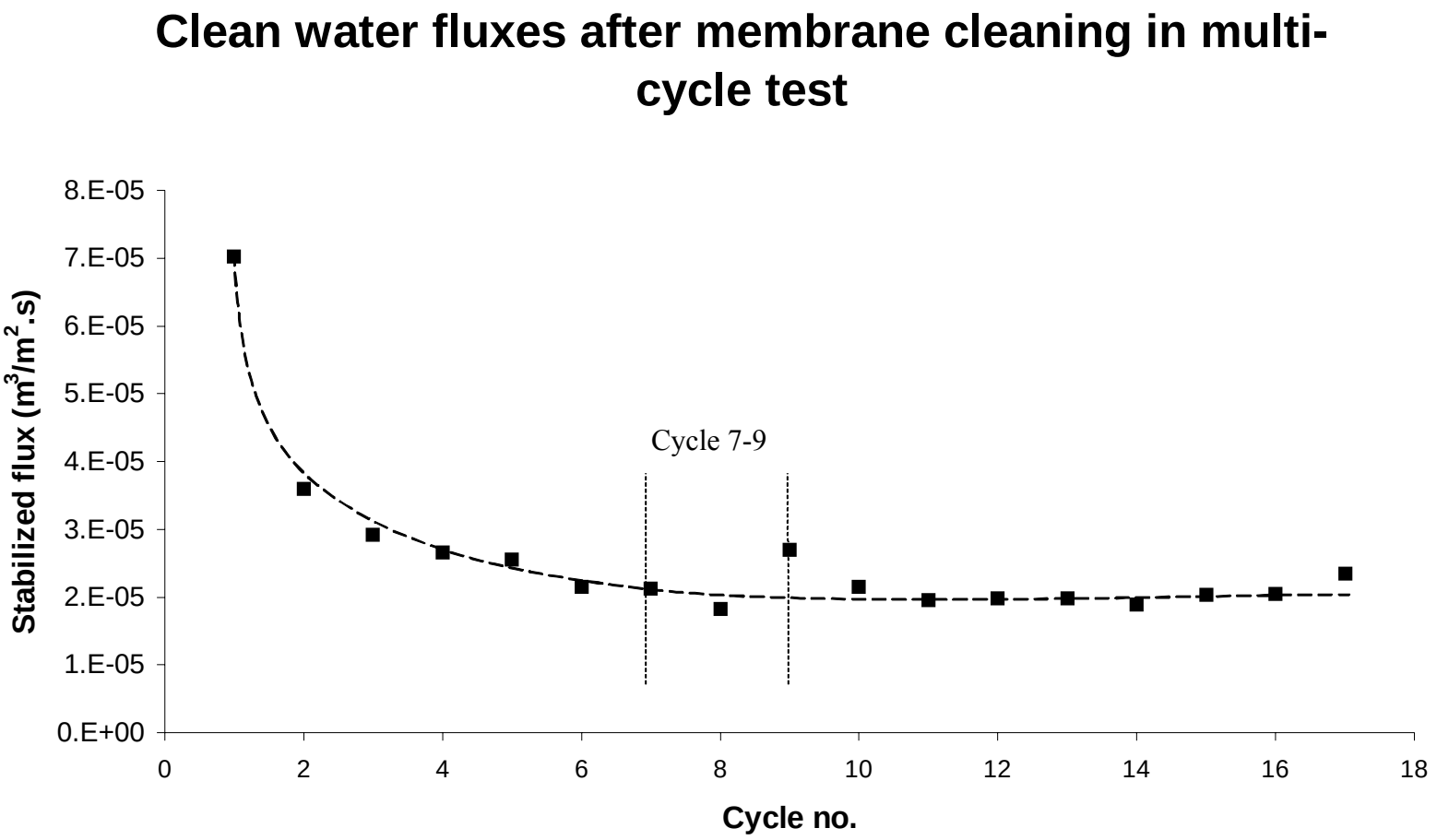

Figure 21 Summary of variation of stabilized clean water fluxes after membrane surface cleaning in the multi-cycle test. The dotted line was added as trend lines.

As shown in Figure 20 and Table 10, the irreversible resistance (R_i) and its significance calculated by dividing R_i by R_t (total resistance) were increasing gradually in the first 5 or 6 cycles and then basically reached a plateau, which was around 20-22% of the total resistance. This was also shown in Figure 21 where the stabilized flux of clean water filtration in step 3 declined from 7.02E-5 m3/m2.s for cycle 1 to 2.15 E-5 m3/m2.s for cycle 6 gradually, then basically maintained at the level of around 2.0E-5 m3/m2.s. It can be concluded that irreversible resistance defined in this research as the resistance that is not removed by the hot and strong water flushing method, which is caused by surface adsorption, pore blocking and constriction, reaches a constant value after 5-6 cycles under the stirred dead-end filtration condition. One possible explanation of this phenomenon is that a sticky skin layer attached onto the membrane surface cannot easily be removed by surface water flushing and this layer will gradually accumulate and be compacted, and reach a maximum while the deposited cake layer above the skin layer, however, can be flushed away during the cleaning procedure.

The control 1 (a new piece of membrane was soaked in DI water, and its clean water permeability was tested after 1, 3 and 11 days of soak respectively) indicated that soaking membrane in DI water did not influence its permeability (Figure 22). The cleaning process of hot (53^{o}C) and strong water flushing (control 2) resulted in slightly adverse effect on the permeability by a 36% decrease after accumulative 90 minute flushing, which was equal to nine times of the cleaning process used in the step 3 of the 3-step test (Figure 23). The reason resulting in the flux decrease in control 2 was unknown. However, this cleaning method was regarded to be applicable to the membrane since the maximum operating temperature of the membrane was 88 ^{o}C according to its technical specification.

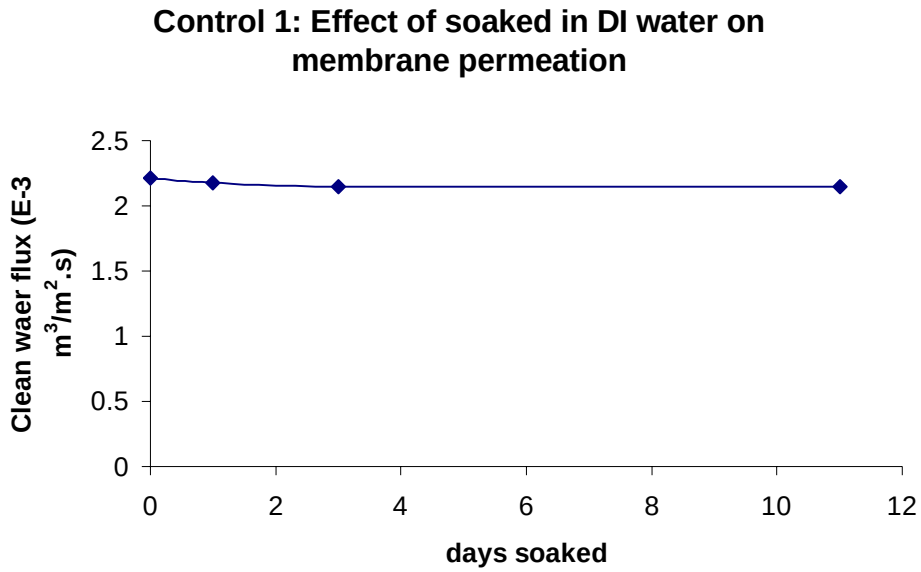

Figure 22 Control 1 – Effect of soaking a new piece of membrane in DI water on its permeation

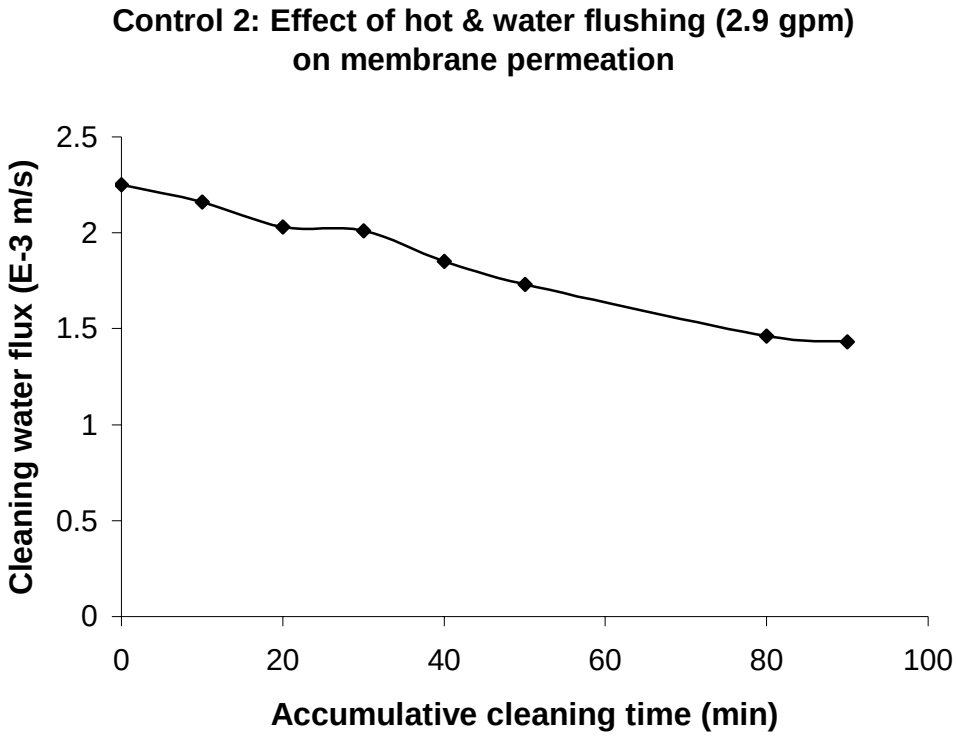

Figure 23 Control 2 – effect of the cleaning method of hot (53^{o}C) and water flushing (2.9 gpm) on membrane permeation. The abscissa is the accumulative time of water flushing. For example, the 2nd point (t = 10 min) means the membrane was flushed for 10 min for the first time, the 7th point (t = 80 min) means a continuous 30 minutes flushing was applied.

3.6 COMPARISON BETWEEN EXPERIMENTAL DATA AND THE LITERATURE

The objective of this section is to investigate whether there is any correlation between sewage effluent filtration and activated sludge dewatering in terms of specific cake resistance and compressibility index n. According to the literature, specific cake resistance is in the magnitude of 10^{12} m/kg for activated sludge [Sorenson and Sorensen, 1997, Rehmat, et al., 1997, Vesilind, 1974]. Specific cake resistance (α) can be used to characterize dewaterability, the higher it is, the more difficult it is to dewater the sludge [Rehmat, et al., 1997].

Waste activated sludge is difficult to dewater and typically the addition of primary sludge and polymeric coagulant and flocculant is a common practice prior to application of pressure or vacuum filtration. The function of coagulant and flocculant addition is to reduce zeta potential close to zero or suppress the electrical charge on the surfaces of the sludge particles. This will allow them to flocculate into larger flocs and the associated specific cake resistance (α) will be reduced. According to Surucu and Cetin's study [1989], α of dispersed sludge is in the magnitude of 10^{15} m/kg, which is much higher than that of flocculated sludge.

Since the particles in primary or secondary effluent are dispersed microorganisms rather than flocculated flocs like activated sludge, the finding in this study that the specific cake resistance of the particles in the sewage effluents ranging in the magnitude of 10^{15} m/kg was reasonable.
The compressibility of the particles in the sewage effluents measured in this study, i.e. 0.56 for primary effluent and 0.45 for secondary effluent, also fall into the range of reported values of activated sludge.

The finding in this study that removable cake resistance (R_c) dominated the total hydraulic resistance of sewage effluent microfiltration is consistent with the claim by Chang, et al. [2001] that cake resistance was more significant than irreversible resistance (R_i) in membrane filtration of activated sludge using ultrafiltration membranes.

In summary (Table 12), the data of specific cake resistance, compressibility index n, and resistance fractionation for sewage effluent filtration in this research agreed closely to the relevant published studies.

Table 12 Comparison of published sludge filtration data with this study

Items		Published data for activated sludge dewatering	Primary/secondary effluent microfiltration in this study
Specific cake resistance	Well flocculated activated sludge	10^{12} m/kg [Sorenson and Sorensen, 1997, Rehmat, et al., 1997, Vesilind, 1974]	10^{15} m/kg (particles in primary/secondary effluent)
	Dispersed solids	10^{15} m/kg [Surucu and Cetin, 1989]	
Compressibility Index n		0.4-0.85 [Vesilind, 1974]	0.56 for particles in primary effluent; 0.45 for particles in secondary effluent
Resistance fractionation		$R_c > R_i$ [Chang, et al., 2001]	▪ $R_c \approx$ 70-80 % of R_t for primary effluent and ≈ 85% for secondary effluent measure by method 1* ▪ $R_c \approx$ 95 % of R_t for primary effluent measured by method 2**

Note: R_c – cake resistance, R_i – irreversible resistance, R_t – total resistance

* The 3-step test procedure described in section 2.6, i.e. clean water filtration – feed water filtration – clean water filtration after membrane cleaning by warm (38 ^oC) and moderate tap water (about 1.5 GPM) flushing for 10 min

** the same as method 1 except the use of adjusted membrane cleaning method, i.e. hotter (53 ^oC) and tap water (about 2.9 GPM) flushing for 10 min

4.0 SUMMARY AND CONCLUSIONS

This study is an extension of a previous research [Modise, 2003] on application of microfiltration of diluted primary and secondary effluents. The main objective of this study is to give a better understanding and quantification of the membrane fouling in treating sewage effluent from municipal wastewater treatment plants. Results from this work can be applied to describe similar microfiltration of combined sewage overflow caused when rainwater and sewage are mixed within a sewer system. In addition, comparisons between microfiltration of primary and secondary effluent filtration and a tap water sample were also made.

A 3-step experimental method using a stirred dead-end cell configuration was developed to define various hydraulic resistances including R_m (resistance of new membrane), R_c (deposited cake resistance) and R_i (resistance which can not be removed by washing and likely caused by irreversibly adsorbed layer, pore blocking and/or constriction), and their respective importance in the fouling of membranes. Briefly, the experimental procedure included i) DI water was filtered through a clean membrane, ii) the feedwater was filtered until flux stabilizes, and iii) the fouled membrane was washed by tap water flushing for 10 min then rinsed with DI water to remove the deposited cake layer, and DI water flux was tested again. The two types of membranes used in this experiment were Pall Versapor and Supor, both of which are hydrophilic 0.2 μm membranes without pre-coating.

More aggressive cleaning methods removed more foulants, however physical abrasion techniques may damage the membrane surface. The optimum membrane cleaning method was determined to be hotter (53 ^{o}C) tap water flushing at a flow rate about 3.6 m^3/m^2.s (2.9 GPM) for 10 min. The 3-step test procedure was correspondingly modified by adopting this cleaning method.

A multiple cycle test, i.e. repeated cycles of filtering primary effluent until flux diminished severely reaching a relative steady state followed by cleaning the membrane surface by water flushing to restore the flux, was conducted to investigate how the irreversible resistance of primary effluent microfiltration would vary over a long-term operation. The adjusted membrane cleaning method was used to remove deposited cake layer after each cycle.

The following conclusions can be drawn from this study:

1) The reversible cake layer resistance (R_c) play a major role in the total hydraulic resistance (R_t) in the microfiltration of both primary effluent and secondary effluent. Therefore, cake resistance was the dominant fouling mechanism. In secondary effluent filtration, the proportion of R_c to R_t is somewhat higher than primary effluent microfiltration.
2) There was no obvious difference in the fouling pattern between the filtration of secondary effluent sampled in a wet weather day and a dry weather day. It may indicate that the fouling pattern is particle characteristics related rather than particle concentration related.
3) The specific cake resistance (α) of primary effluent ranged in 1.8-2.7 $*10^{15}$ m/kg at the pressure of 10-20 psi, while α of secondary effluent was in the range of 3.3 – 4.5 $*10^{15}$ m/kg in the same pressure range. This is in consistence with the statement in literature

that primary sludge has comparatively lower α than secondary sludge. The compressibility index n was 0.56 for primary effluent solids, and 0.45 for secondary effluent solids, suggesting that the suspended solids in sewage effluents were compressible. The magnitude of this specific cake resistance of particles in both primary and secondary effluent, i.e. 10^{15} m/kg, is consistent with published data for dispersed activated sludge, while well flocculated sludge would be in the magnitude of 10^{12} m/kg.

4) The tap water taken from the lab at University of Pittsburgh showed a totally different fouling pattern. Irreversible resistance (R_i) occupied 74% of total resistance (R_t), becoming the major resistance, while cake resistance (R_c) was only 3% of R_t.

5) The significant difference of fouling pattern between sewage effluent and tap water, and the finding that R_c / R_t in secondary effluent filtration is higher than that in primary effluent filtration suggest that the deposited cake properties and fouling mechanism are related to the characteristics of the particles in the feed water. It may indicate that cakes formed by inorganic particles are hard to remove, and cakes containing microbial flocs are more removable.

6) The irreversible resistance in microfiltration of primary effluent gradually increased from an initial 5% to about 21% of total resistance after six cycles and then basically remained constant at this plateau. This finding is significant to the environmental engineering design of microfiltration systems for the production of clean water and management of wastewater.

5.0 SUGGESTIONS FOR FURTHER STUDIES

The most important impediment of membrane filtration is the permeate flux decline due to membrane fouling. The most challenging part of fouling is the irreversible adsorption of substances onto or into the membrane. The general improvement methods of membrane performance can be classified into four categories: pretreatment of feed solution, adjustment of membrane materials properties, membrane cleaning and improvement of operating conditions [Park, 2002]. Except for membrane cleaning, the other three categories are preventative means. Further studies of this work should be focused on these preventative anti-fouling technologies.

Coagulation pretreatment is known to reduce the rate of fouling of microfiltration, possibly by aggregating fine particles to increase cake permeability or prevent pore blockage, conditioning of the cake by incorporation of fine particles into highly-porous flocs, or precipitation or adsorption of dissolved materials into flocs [Wiesner and Lanine, 1996]. Internal back washing by ozone gas was proved effective for flux recovery in microfiltration of municipal raw sewage. It may be attributed to the removal of foulants attached on the surface and in the membrane pores by 1) decomposition of organic foulants by ozonation and 2) physical tangential force [Kim, et al. 2002]. A new technology is pulsed blackbody radiation flux enhancement [Bender, 2003]. Its core technology is the pulsed blackbody UV (PBUV, marked by PALL Corp), which yields short lived oxidizing species. It is suggested that this results in precipitation of inorganic molecules or organically complexed minerals, partial or complete mineralization of organic molecules and deactivation or destruction of microbes including virus, bacteria and protozoa. Bender's patent

shows that a pretreatment of PBUV results in an enhanced overall flux through the membranes. This technology can reduce transmembrane pressure (TMP) and the duration of backwash and caustic cleaning cycles. Fe and Mn turn into hydroxide crystals trapped by the membrane and separated from the permeate. This may indicate a very promising technology to minimize fouling and improve the membrane performance.

Based on abovementioned findings from literatures, a further study is proposed mainly based on PBUV and other potentially beneficial pretreatment means to reduce membrane fouling in microfiltration, especially irreversible fouling. The starting point will be an investigation whether the PBUV pretreatment or PBVU + coagulation technique can mitigate downstream membrane fouling. If it works, further more fundamental studies on the change of water chemistry, molecular weight distribution of the macromolecules, as well as the properties of the cake layer and the irreversible fouling, etc. should be ensued aiming at investigate the principle of the anti-fouling effect. Another possible improvement on design may be incorporating ozone gas backpulsing into the membrane module to investigate whether additional benefit in terms of fouling reduction will be achieved.

APPENDIX A

DERIVATIONS OF W AND α

Derivation of w, cake deposited per volume of filtrate

Vacuum filtration for sludge

Liquid balance: $V_b = V_f + V_c$

And solids balance yields: $V_bC_b = V_fC_f + V_cC_c$

Where V is volume and C is solids concentration, and the subscripts b, f and c denote feed, filtrate and cake, respectively.

The weight of dry solids deposited as cake per volume of filtrate, defined as w, is

$$w = \frac{V_c C_c}{V_f}$$

Substituting from the liquid balance above,

$$w = \frac{(V_b - V_f)C_c}{V_f}$$

rearranging the liquid balance and substituting,

$$V_f C_f = V_b C_b - V_c C_c$$
$$V_f C_f = V_b C_b - (V_b - V_f) C_c$$
$$V_f C_f - V_f C_c = V_b C_b - V_b C_c$$
$$V_f = \frac{V_b (C_b - C_c)}{C_f - C_c}$$

Substituting

$$w = \frac{V_b C_c - [\frac{V_b (C_b - C_c)}{C_f - C_c}] C_c}{\frac{V_b (C_b - C_c)}{C_f - C_c}}$$

Assuming $C_f = 0$,

$$w = \frac{C_c C_b}{C_c - C_b}$$

$\because Cc >> C_b$, assuming C_b is negligible compared with C_c,

$\therefore w \approx C_b$

Derivation of specific cake resistance (α)

Using Darcy's law:

$$\frac{dV}{dt} = \frac{PA}{\mu R}$$

In a filter, resistance is contributed by both filter medium and cake,

$$\frac{dV}{dt} = \frac{P}{\mu} \frac{A}{(\delta R_c + R_m)}$$

where δ = cake thickness

The volume of cake can be expressed as

$$\delta A = vV$$

where v = volume of cake deposited per unit volume of filtrate.

Substituting,

$$\frac{dV}{dt} = \frac{pA^2}{\mu(R_c vV + R_m A)}$$

It's more convenient to express cake as dry weight /volume instead of vol of cake /vol of filtrate.

Also, R_c (resistance by a unit volume) is replaced by α, resistance by unit weight. Thus,

$$\frac{dV}{dt} = \frac{pA^2}{\mu(w\alpha V + R_m A)}$$

$\because$ P is constant over time,

$$\therefore \int_0^t dt = \int_0^V (\frac{\mu w \alpha V}{PA^2} + \frac{R_m \mu}{PA})dV$$

$$\therefore t = \frac{\mu w \alpha V^2}{2PA^2} + \frac{R_m \mu V}{PA} or \frac{t}{V} = \frac{\mu \alpha w V}{2PA^2} + \frac{\mu R_m}{PA}$$

where it is assumed that w is kept constant during filtration.

The above equation is a straight line of type of y =bx +a, where,

$$b = \frac{\mu \alpha w}{2PA^2}$$

$$\therefore \alpha = \frac{2PA^2 b}{\mu w}$$

$\because w \approx C_b$

$$\therefore \alpha = \frac{2PA^2 b}{\mu C_b}$$

Compressibility index, n

$$\alpha = \alpha_0 \Delta P^n$$

n is the slope on a log-log plot, indicating how much the solids are compressed. “n” varies from 0 for rigid incompressible cakes to 1.0 for compressible cakes to greater than 1.0 for highly compressible cakes [Ho and Sirkar, 1992]. Incompressible materials like sand, would have n=0. For domestic sludge, n has been found to range between 0.4 to 0.85 [Vesilind, 1974].

APPENDIX B

SAMPLE CALCULATION OF THE FLUX RESISTANCES IN THE 3-STEP TEST

Using a part of Table 2 as an example

Membrane	Step	Stabilized flux, J_v ($m^3/m^2.s$)	Hydraulic resistance (m^{-1})		Contribution to the R_t (%)
Versapor	1	1.42E-03	R_m	7.27E+10	0.28%
	2	4.01E-06	R_t	2.58E+13	-
	3	1.46E-05	R_c	1.87E+13	72.6%
			R_i	7.00E+12	27.1%

$$R_m = \frac{\Delta P}{J_{v1} \times \eta_w} = \frac{15\,psi * 6.8948 * 10^3\,Pa/psi}{1.42 * 10^{-3}\,m/s * 1.002 * 10^{-3}\,Pa.s} = 7.27 * 10^{10}\,m^{-1}$$

$$R_t \equiv R_m + R_c + R_i = \frac{\Delta P}{J_{v2} \times \eta_w} = \frac{103422\,Pa}{4.01 * 10^{-6}/s * 1.002 * 10^{-3}\,Pa.s} = 2.58 * 10^{13}\,m^{-1}$$

$$R_i + R_m = \frac{\Delta P}{J_{v3} \times \eta_w} = \frac{103422\,Pa}{1.46 * 10^{-5}\,m/s * 1.002 * 10^{-3}\,Pa.s} = 7.07 * 10^{12}\,m^{-1}$$

$\therefore$ $R_i = (R_i + R_m) - R_m = 7.00 * 10^{12}\ m^{-1}$

$R_c = R_t - (R_i + R_m) = 1.87 * 10^{13}\ m^{-1}$

APPENDIX C

MEASUREMENT OF SPECIFIC CAKE RESISTANCE (α) FOR PRIMARY EFFLUENT

Table 13 Raw data of filtration of primary effluent with transmembrane pressure of 10 psi

W (g)	t (s)	V (m^3)	t/V (s/m^3)
20	13.6	0.000020	680000
60	139	0.000060	2316667
90	346	0.000090	3844444
119	635	0.000119	5336134
161	1216	0.000161	7552795
194	1815	0.000194	9355670
236	2818	0.000236	11940678
256	3354	0.000256	13101563
283	4154	0.000283	14678445
315	5225	0.000315	16587302
333	5885	0.000333	17672673
351	6590	0.000351	18774929
367	7255	0.000367	19768392

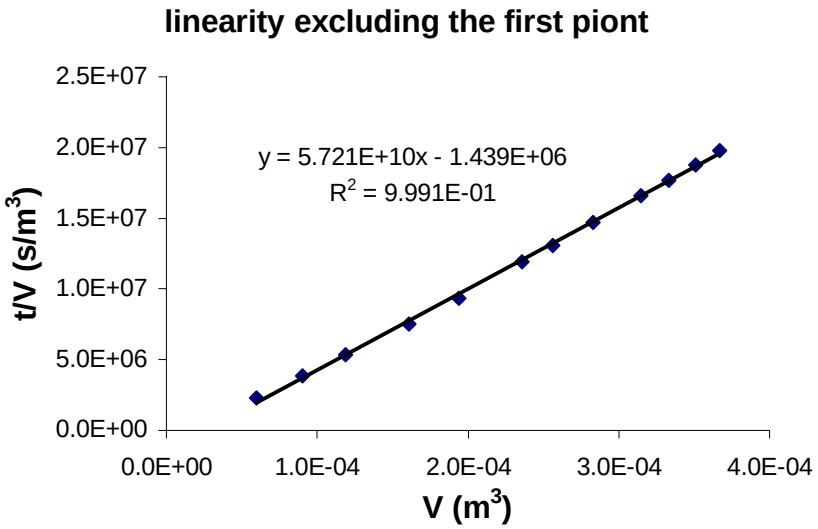

Figure 24 Plotting t/V vs. V to get the slop of the linear phase, which is used to calculate the specific cake resistance α_{10psi} for primary effluent according to the equation $\alpha = \frac{slope \times 2A^2 \Delta P}{\mu C_b}$.

Table 14 Raw data of filtration of primary effluent with transmembrane pressure of 15 psi

W (g)	t (s)	V (m^3)	t/V (s/m^3)
20	14.9	0.000020	745000
60	106	0.000060	1766667
92	302	0.000092	3282609
130	685	0.000130	5269231
168	1243	0.000168	7398810
208	1921	0.000208	9235577
238	2538	0.000238	10663866
263	3118	0.000263	11855513
283	3631	0.000283	12830389
311	4414	0.000311	14192926
331	5019	0.000331	15163142
350	5638	0.000350	16108571
370	6320	0.000370	17081081
387	6940	0.000387	17932817

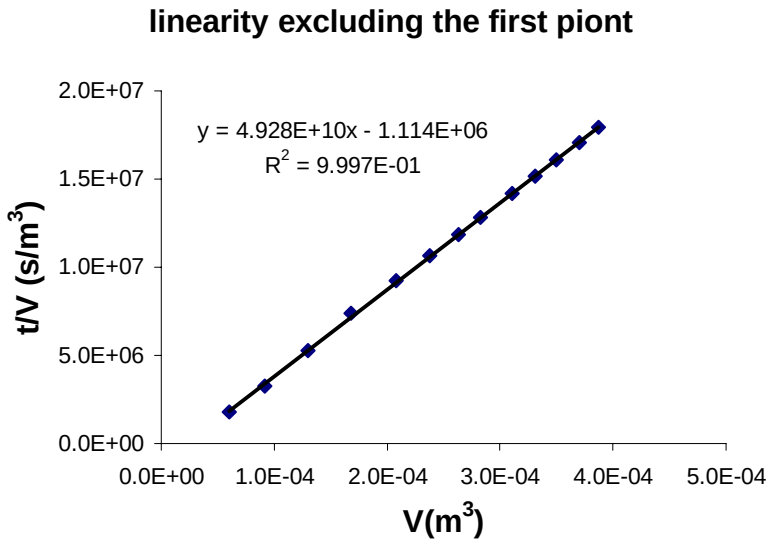

Figure 25 Plotting t/V vs. V to get the slop of the linear phase, which is used to calculate the specific cake resistance α_{15psi} for primary effluent according to the equation $\alpha = \frac{slope \times 2A^2 \Delta P}{\mu C_b}$.

Table 15 Raw data of filtration of primary effluent with transmembrane pressure of 20 psi

W (g)	t (s)	V (m^3)	t/V (s/m^3)
20	21.4	0.000020	1070000
60	100	0.000060	1666667
107	362	0.000107	3383178
157	841	0.000157	5356688
212	1611	0.000212	7599057
248	2255	0.000248	9092742
276	2835	0.000276	10271739
306	3540	0.000306	11568627
343	4524	0.000343	13189504
365	5173	0.000365	14172603
388	5912	0.000388	15237113
406	6528	0.000406	16078818
423	7142	0.000423	16884161

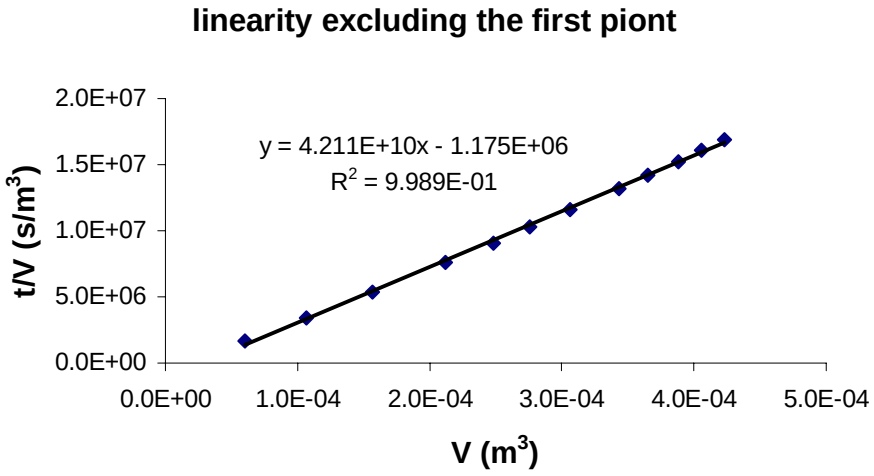

Figure 26 Plotting t/V vs. V to get the slop of the linear phase, which is used to calculate the specific cake resistance α_{20psi} for primary effluent according to the equation $\alpha = \frac{slope \times 2A^2 \Delta P}{\mu C_b}$.

Demonstrating Calculation of Calculating Specific Cake Resistance α for primary effluent

$$\alpha_{10\,psi} = \frac{2PA^2 \times slope}{\mu \times C_b}$$

$$= \frac{2 \times 10\,psi \times 6.8948 \times 10^3\,(Pa/psi) \times (3.85 \times 10^{-3}\,m^2)^2 \times 5.721 \times 10^{10}\,s/m^6}{1.002 \times 10^{-3}\,Pa.s \times 6.4 \times 10^{-2}\,kg/m^3}$$

$$= 1.82 \times 10^{15}\,m/kg$$

where, C_b (SS concentration in the primary effluent) = 6.4 *10^{-2} kg/m^3

APPENDIX D

MEASUREMENT OF SPECIFIC CAKE RESISTANCE (α) FOR SECONDARY EFFLUENT

Table 16 Raw data of filtration of secondary effluent with transmembrane pressure of 10 psi

Weight (g)	time (s)	time (min)	V (m^3)	t/V (s/m^3)
20	14.5	0.2	2.00E-05	7.25E+05
50	36.8	0.6	5.00E-05	7.36E+05
115	126	2.1	1.15E-04	1.10E+06
200	395	6.6	2.00E-04	1.98E+06
270	841	14.0	2.70E-04	3.11E+06
340	1483	24.7	3.40E-04	4.36E+06
403	2218	37.0	4.03E-04	5.50E+06
465	3074	51.2	4.65E-04	6.61E+06
514	3844	64.1	5.14E-04	7.48E+06
554	4531	75.5	5.54E-04	8.18E+06
596	5313	88.6	5.96E-04	8.91E+06
627	5930	98.8	6.27E-04	9.46E+06
655	6516	108.6	6.55E-04	9.95E+06
682	7103	118.4	6.82E-04	1.04E+07

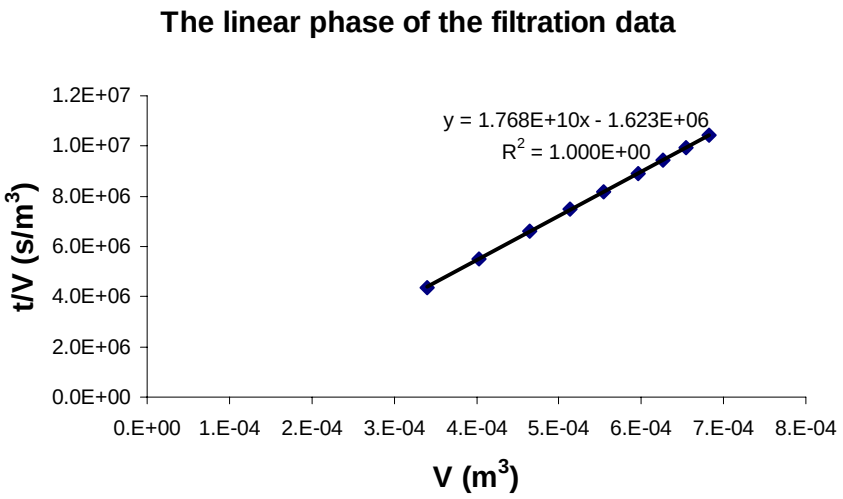

Figure 27 Plotting t/V vs. V to get the slop of the linear phase, which is used to calculate the specific cake resistance α_{10psi} for secondary effluent according to the equation $\alpha = \frac{slope \times 2A^2 \Delta P}{\mu C_b}$.

Table 17 Raw data of filtration of secondary effluent with transmembrane pressure of 15 psi

Weight (g)	time (s)	time (min)	V (m^3)	t/V (s/m^3)
20	14.5	0.2	2.00E-05	7.25E+05
50	36.8	0.6	5.00E-05	7.36E+05
115	126	2.1	1.15E-04	1.10E+06
200	395	6.6	2.00E-04	1.98E+06
270	841	14.0	2.70E-04	3.11E+06
340	1483	24.7	3.40E-04	4.36E+06
403	2218	37.0	4.03E-04	5.50E+06
465	3074	51.2	4.65E-04	6.61E+06
514	3844	64.1	5.14E-04	7.48E+06
554	4531	75.5	5.54E-04	8.18E+06
596	5313	88.6	5.96E-04	8.91E+06
627	5930	98.8	6.27E-04	9.46E+06
655	6516	108.6	6.55E-04	9.95E+06
682	7103	118.4	6.82E-04	1.04E+07

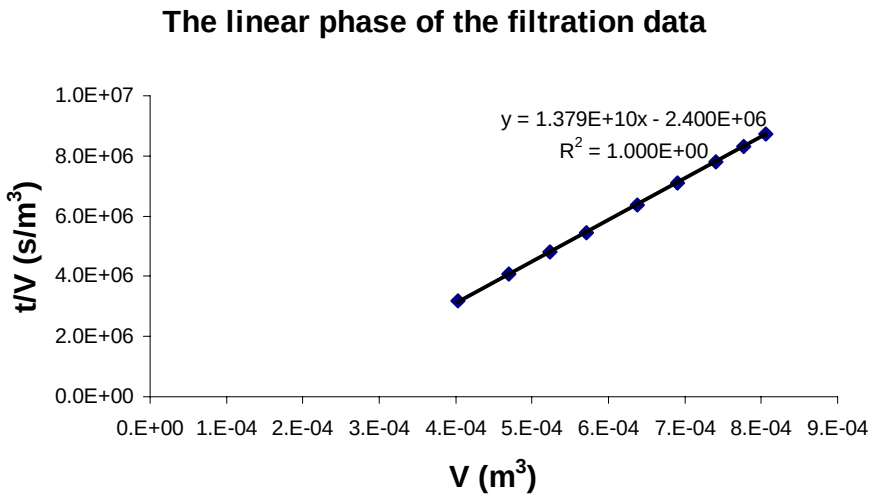

Figure 28 Plotting t/V vs. V to get the slop of the linear phase, which is used to calculate the specific cake resistance α_{15psi} for secondary effluent according to the equation $\alpha = \frac{slope \times 2A^2 \Delta P}{\mu C_b}$.

Table 18 Raw data of filtration of secondary effluent with transmembrane pressure of 20 psi

Weight (g)	time (s)	time (min)	V (m^3)	t/V (s/m^3)
60	13.8	0.2	6.00E-05	2.30E+05
100	26.2	0.4	1.00E-04	2.62E+05
200	89	1.5	2.00E-04	4.45E+05
307	312	5.2	3.07E-04	1.02E+06
402	802	13.4	4.02E-04	2.00E+06
488	1459	24.3	4.88E-04	2.99E+06
566	2218	37.0	5.66E-04	3.92E+06
629	2940	49.0	6.29E-04	4.67E+06
758	4723	78.7	7.58E-04	6.23E+06
806	5494	91.6	8.06E-04	6.82E+06
843	6126	102.1	8.43E-04	7.27E+06
893	7039	117.3	8.93E-04	7.88E+06

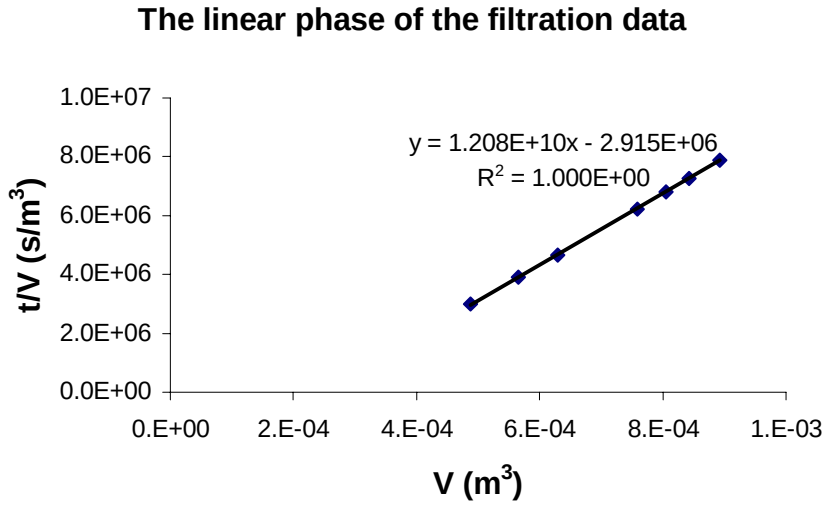

Figure 29 Plotting t/V vs. V to get the slop of the linear phase, which is used to calculate the specific cake resistance α_{20psi} for secondary effluent according to the equation $\alpha = \frac{slope \times 2A^2 \Delta P}{\mu C_b}$.

Demonstrating Calculation of Calculating Specific Cake Resistance α for secondary effluent

$$\alpha_{10\,psi} = \frac{2PA^2 \times slope}{\mu \times C_b}$$

$$= \frac{2 \times 10\,psi \times 6.8948 \times 10^3 (Pa/psi) \times (3.85 \times 10^{-3} m^2)^2 \times 1.768 \times 10^{10} s/m^6}{1.002 \times 10^{-3} Pa.s \times 11 \times 10^{-3} kg/m^3}$$

$$= 3.28 \times 10^{15} m/kg$$

where, C_b (SS concentration in the secondary effluent) = 11 $*10^{-3}$ kg/m^3

APPENDIX E

INFLUENCE OF PHYSICAL ABRASION OF MEMBRANE ON RESTORING PERMEATE FLUX

Cleaning methods	Stabilized flux, J_v ($m^3/m^2.s$)		R_t (total resistance, m^{-1})	R_i (irreversible resistance, m^{-1})		R_c (cake resistance, m^{-1})	
	Step 2* (J_{v2})	Step 3* (J_{v3})		Value	% of R_t	Value	% of R_t
1. Warm (38 ^oC) and moderate tap water (about 1.9 $m^3/m^2.s$) flushing for 10 min	3.79E-6	2.16E-5	2.72E13	4.73E12	17.4	2.24E13	82.4
2. Hotter (53 ^oC) and strong tap water (about 3.6 $m^3/m^2.s$) flushing for 10 min	3.77E-6	7.02E-5	2.74E13	1.42E12	5.2	2.59E13	94.6
3. Gentle scrubbing with toothbrush	3.69E-6	1.91E-4	2.80E13	4.93E11	1.76	2.75E13	98.07
4. Gentle scraping with blade	3.68E-6	1.20E-4	2.80E13	8.13E11	2.9	2.71E13	96.9

Note: J_{v1} = 2.20E-3 $m^3/m^2.s$, R_m (membrane resistance) = 4.69E10 m^{-1}.

* 3-step test: I. DI water filtration; II. feed water filtration; III. DI water filtration after membrane surface cleaning by the above four different methods and then rinsed with DI water to remove the deposited cake layer.

BIBLIOGRAPHY

Abdessemed D. and Nezzal G. (2002) Treatment of primary effluent by coagulation-adsorption-ultrafiltration for reuse, Desalination, 152, 367-373

Ahn K. and Song K. (1999) Treatment of domestic wastewater using microfiltration for reuse of wastewater, Desalination 126, 7-14

Alonso E., et al. (2001) On the feasibility of urban wastewater tertiary treatment by membranes: a comparative assessment, Desalination, 141, 39-51

Arnot T. C., et al. (2000) Cross-flow and dead-end microfiltration of oily-water emulsions Part II. Mechanisms and modeling of flux decline, J. Mem. Sci., 169, 1-15

Bender J., (2003) Pulsed blackbody radiation flux enhancement, US Patent No. 200030102269

Benkahla Y. K., et al. (1995) Cake growth mechanism in cross-flow microfiltration of mineral suspensions, J. Mem. Sci. 98, 107-117

Boerlage S. F. E., et al. (1998) Monitoring particulate fouling in membrane systems, Desalination 118, 131-142

Boerlage S. F. E., et al. (2003) The MFI-UF as water quality test and monitor, J. Mem. Sci. 211, 271-289

Bourgeous K. N., et al. (2001) Ultrafiltration of wastewater: effects of particles, mode of operation, and backwash effectiveness, Wat. Res., Vol. 35, No. 1, 77-90

Cardew P. T. and Le M. S. (1998) Membrane processes: a technology guide, North West Water Ltd,

Carman, P. C. (1938) Fundamental principles of industrial filtration, Trans. Inst. Chem. Eng., 16, 168-176

Chang I, Bag S, and Lee C (2001) Effects of membrane fouling on solute rejection during membrane filtration of activated sludge, Process Biochemistry, 36, 8-9, 855-860

Chang I., et al. (1999) Membrane filtration characteristics in membrane-coupled activated sludge system: the effect of floc structure on membrane fouling, Separation Sci. and Tech. 34 (9), 1743-1758

Chang I., et al. (2002) Membrane fouling in membrane bioreactors for wastewater treatment, J. of Env. Eng., Nov., 1018-1029

Choi J., et al. (2002) The behavior of membrane fouling initiation on the crossflow membrane bioreactor system, J. Mem. Sci. 203, 103-113

Chudacek M. W. and Fane A. G. (1984) The dynamics of polarization in unstirred and stirred ultrafiltration, J. of Mem. Sci., 21, 145-160

Defrance L. and Jaffrin M. Y. (1999) Comparison between filtrations at fixed transmembrane pressure and fixed permeate flux: application to a membrane bioreactor for wastewater treatment, J Mem. Sci. 152, 203-210

Defrance L. and Jaffrin M. Y. (1999) reversibility of fouling formed in activated sludge filtration, J. of Mem. Sci., 157, 73-84

EPA/625/R-92/001 (1992) Control of biofilm growth in drinking water distribution systems, Washington, DC: Office of Research and Development

Field R. W. et al. (1995) Critical flux concept for microfiltration fouling, J. of Mem. Sci., 100, 259-272

Gesan-Guiziou G., et al. (1999) Critical stability conditions in crossflow microfiltration of skimmed milk: transition to irreversible deposition, J Mem. Sci., 158, 211-222

Grace H. P. (1953) Resistance and compressibility of filter cake, Chem. Eng. Prog. 49, 303-318

Gulas V, Bond M, and Benefield L (1979) Use of exocellular polymers for thickening and dewatering activated sludge, J Wat. Pollut. Control Fed., 51, 798

Hjortso M. A. and Roos J. W. (1995) Cell adhesion: fundamentals and biotechnological applications, New York: M. Dekker

Ho W. S. W. and Sirkar K. K. (1992) Membrane handbook, Van Nostrand Reinhold, New York

Howe K. J. and Clark M. M. (2002) Fouling of microfiltration and ultrafiltration membranes by natural waters, Environ. Sci. Technol. 36, 3571-3576

Hsieh H. P. (1996) Inorganic membranes for separation and reaction, Elsevier

Hwang K. and Hsueh C. (2003) Dynamic analysis of cake properties in microfiltration soft colloids, J. Mem. Sci., 214, 259-273

Jiraratananon R. and Chanachai A. (1996) A study of fouling in the ultrafiltration of passion fruit juice, J. Mem. Sci., 111, 39-48

Kang I., et al. (2003) Characteristics of microfiltration membranes in a membrane coupled sequencing batch reactor system, Wat. Res. 37, 1192-1197

Kwak S. and Kim S (2001) Hybrid organic/inorganic reverse osmosis (RO) membrane for bacterial anti-fouling, Env. Sci. Tech., 35, 2388-2394

Lee J. et al (2001) Comparison of the filtration characteristics between attached and suspended growth microorganisms in submerged membrane bioreactor, Wat. Res. 35(10), 2435-2445

Lu W., et al. (2001) Constant pressure filtration of mono-dispersed deformable particle slurry, Separation Sci. Tech., 36 (11), 2355-2383

Marchese J., et al. (2000) Pilot-scale ultrafiltration of an emulsified oil wastewater, Env. Sci. Tech., 34, 2990-2996

Modise C. M., (2003) Use of polymeric microfiltration membranes to remove microorganisms and organic pollutants from primary sewage effluent, MS Thesis, University of Pittsburgh

Nakanishi K., et al. (1987) On the specific resistance of cakes of microorganisms, Chem. Eng. Comm., 62, 187-201

Ousman M. and Bennasar M. (1995) Determination of various hydraulic resistances during cross-flow filtration of a starch grain suspension through inorganic membranes, J. Mem. Sci., 105, 1-21

Pall website, http://www.pall.com/laboratory.asp

Parameshwaran K., et al. (2001) Analysis of microfiltration performance with constant flux processing of secondary effluent, Wat. Res. 35 (18), 4349-4358

Personal communication with a technical consultant of PALL, 2003

Rehmat T, Branion R, S Duff and M Groves (1997) A laboratory sludge press for characterizing sludge dewatering, Wat. Sci. Tech., 35, 2-3, 189-196

Rudie B., Hydrophilicity and hydrophobicity, website of Osmonics, http://www.osmonics.com/products/Page772.htm

Sondhi R., et al. (2000) Crossflow filtration of chromium hydroxide suspension by ceramic membranes: fouling and its minimization by backpulsing, J Mem. Sci. 174, 111-122

Sondhi R. and Bhave R. (2001) Role of backpulsing in fouling minimization in crossflow filtratioln with ceramic membranes, J. of Mem. Sci., 186, 41-52

Sorensen B L and Sorensen P B (1997) Applying cake filtration theory on membrane filtration data, Wat. Res., 31, 3, 665-670

Speth T. F., et al. (1998) Nanofiltration foulants from a treated surface water, Env. Sci. Tech., 32, 3612-3617

Standard Methods for The Examination of Water and Wastewater, 20th edition, AWWA

Surucu G and Cetin F D (1989) Effect of temperature, pH and DO concentration on filterability and compressibility of activated sludge, Wat. Res., 23, 11, 1389-1395

Tardieu E., et al. (1998) Hydrodynamic control of bioparticles in a MBR applied to wastewater treatment, J Mem. Sci. 147, 1-12

Tiller F. M. and Green T. C. (1973) Role of porosity in filtration IX skin effect with highly compressible materials, AIChE J. 19(6), 1266-1269

Tiller F. M. and Kwon J. H. (1998) Role of porosity in filtration: XIII. Behavior of highly compactable cakes, AIChE J. 44 (10), 2159-2167

Tiller F. M. et al. (1980) A revised approach to the theory of cake filtration, in P. Sanasundaran (Ed.), Fine Particles Processes, vol. 2, New York, 1549-1558

Vesilind P A (1974) Treatment and disposal of wastewater sludges, Ann Arbor Science publishers Inc.

Walkers J, et al. (2000) Industrial biofouling: detection, prevention, and control, Chichester, UK, New York, Wiley

Ward A. S. (1988) Liquid filtration theory, Chapter 2, Filtration Principles and practices, 2nd edition, Marcel Dekker Inc.

Zeman L. J. and Zydney A. L. (1996) Microfiltration and ultrafiltration, principles and applications, Marcel Dekker, Inc.

Zhao Y., et al. (2002) Fouling and regeneration of ceramic microfiltration membranes in processing acid wastewater containing fine TiO_2 particles, J. of Mem. Sci., 208, 331-341